Quantification and Quality Control of Extracellular Vesicles Using Capillary Electrophoresis

Yuchu Dou

A thesis submitted in partial fulfillment of the requirements for the degree of

Master of Science

Department of Chemistry and Biomolecular Science
Faculty of Science
University of Ottawa

Table of Contents

List of Figures

List of tables

List of Abbreviations

BCA: Bicinchoninic acid

CE: Capillary electrophoresis

DLS: Dynamic light scattering

DNA: Deoxyribonucleic acid

ELISA: Enzyme-linked immunosorbent assay

EOF: Electroosmotic flow

EVs: Extracellular vesicles

EVqCE: Extracellular vesicles quantitative capillary electrophoresis

FBS: Fetal bovine serum

LIF: laser-induced fluorescence

miRNA: Micro ribonucleic acid

mRNA: Messenger ribonucleic acid

NTA: Nanoparticle tracking analysis

PBS: Dulbecco's phosphate buffered saline

PDA: Photodiode array

qRT-PCR: Real-time polymerase chain reaction

RNA: Ribonucleic acid

SDS: Sodium dodecyl sulphate

SPR: Surface plasmon resonance

TEM: Transmission electron microscopy

TRPS: Tunable resistive pulse sensing

UC: ultracentrifugation

UV-VIS: Ultraviolet–visible

Abstract

Extracellular vesicles (EVs) gained significant interest within the last decade as a new source of biomarkers for the early detection of diseases and as a promising tool for therapeutic applications. As a result, a need for new methods for EV analysis and quantification has elevated. In this work, I apply Extracellular Vesicles Quantitative Capillary Electrophoresis (EVqCE) to determine (i) the apparent molecular weight of RNA in EVs, (ii) the number of intact EVs in a sample, and (iii) the degree of EV degradation after sonication, vortexing, freeze-thaw cycles and long storage. This separation method is demonstrated on EVs isolated from conditioned media of three different cancer cell lines and human urine samples. Here, I utilize capillary zone electrophoresis with laser-induced fluorescent detection to separate intact EVs from DNA and RNA impurities present in the sample. YOYO-1 dye is used to stain all DNA and RNA in the sample. After lysis of EVs with a detergent, encapsulated DNA and RNA are released. After additional RNase treatment of the EVs sample, RNA is enzymatically cleaved, leaving residual DNA only, in order to calculate the RNA concentration from EVs. Therefore, the initial concentration of intact EV is calculated based on the gain of a nucleic acid peak in capillary electrophoresis and an RNA calibration curve. EVqCE works in a dynamic range of EV concentrations from 10^8 to 10^{10} particles/mL. The quantification process can be completed in less than one hour and requires minimum optimization for CE separation.

Acknowledgements

During the preparation of the master's thesis, I have received a lot of invaluable help from many people. Their comments and advice contribute to the accomplishment of the thesis.

First and foremost, profound gratitude should go to my supervisor, Professor Dr. Maxim Berezovski. He is the person who provided me with the chance to proceed to my graduate study in Canada. As the one who opens my gateway to science, he decently instructed me on literature understanding, instrument operation, presentation skills and scientific thinking. His enlightening had not only improved me in my graduate study but also benefited me for the rest of my life.

Secondly, I want to express my heartfelt thanks to my lab members, both past and present. I thank Dr. Shahrokh Ghobadloo for teaching me knowledge regarding flow cytometry. I thank Dr. Zoran Minic for teaching me a mass spectrometry course. I thank Dr. Prabir Kumar Kulabhusan for providing me valuable suggestions and instruction during my project. I would also like to show my appreciation to my co-workers. Lixuan, thank you for the cooperation and help in these two years' program. Nico and Vanessa, I enjoy the time when we struggled together. Emil, Yaroslav, Yousef and Suttinee, thank you for your patience and warm heart. And thanks to all my colleagues for your help during the research, courses, seminar and activities. Your company made me feel so fulfilled and grateful in these years.

Finally, I want to show my appreciation to my family for their support in my study as well as my life. Thank you for always supporting me. In the journey of my life, this period of graduate study is quite an important and unforgettable part.

Statement of contributions

Y. Dou designed and performed the experiments, data analysis, wrote the thesis, L. Ren helped in the experiments with EVs from cell media, in discussion and troubleshooting. P. K. Kulabhusan taught me how to do cell culturing and EV isolation. S. Ghobadloo helped me in flow cytometry tests and data analysis. M. Berezovski supervised my work, conceptualized experiments, helped in CE analysis, draft correction and funding acquisition.

Chapter 1. Introduction

1.1 Extracellular vesicles

1.1.1 Overview

Extracellular vesicles (EVs) are biological nano-sized particles released from various cells and found in large numbers in the body fluid, including blood, saliva, amniotic fluid, and urine. Most EVs present in body fluid samples are hollow vesicle structure consisting of a large variety of molecular constituents like lipids, proteins, and genetic material (mRNA, miRNA, DNA), delimited by a phospholipid bilayer. EVs have a diameter range from 50–1,000 nm, which can be distinguished as three broad classes including exosomes (50–150 nm, originating from the endosomal pathway) and microvesicles (100 - 1,000 nm, released from the plasma membrane) and apoptotic bodies(>1000 nm, budded during cell death).[1-4] While these definitions hold in theory, in practice, it is difficult to properly isolate different sub-categories of EVS since the collected samples contain heterogeneous EV- suspensions. The significant overlap in size, similarities in composition and lack of specific surface biomarkers has made their classification an extremely challenging experimental task, and the terminology in the current literature is often confusing and ambiguous.[5] Therefore, in this study, I mainly used the more generic term, i.e., extracellular vesicles (EVs).

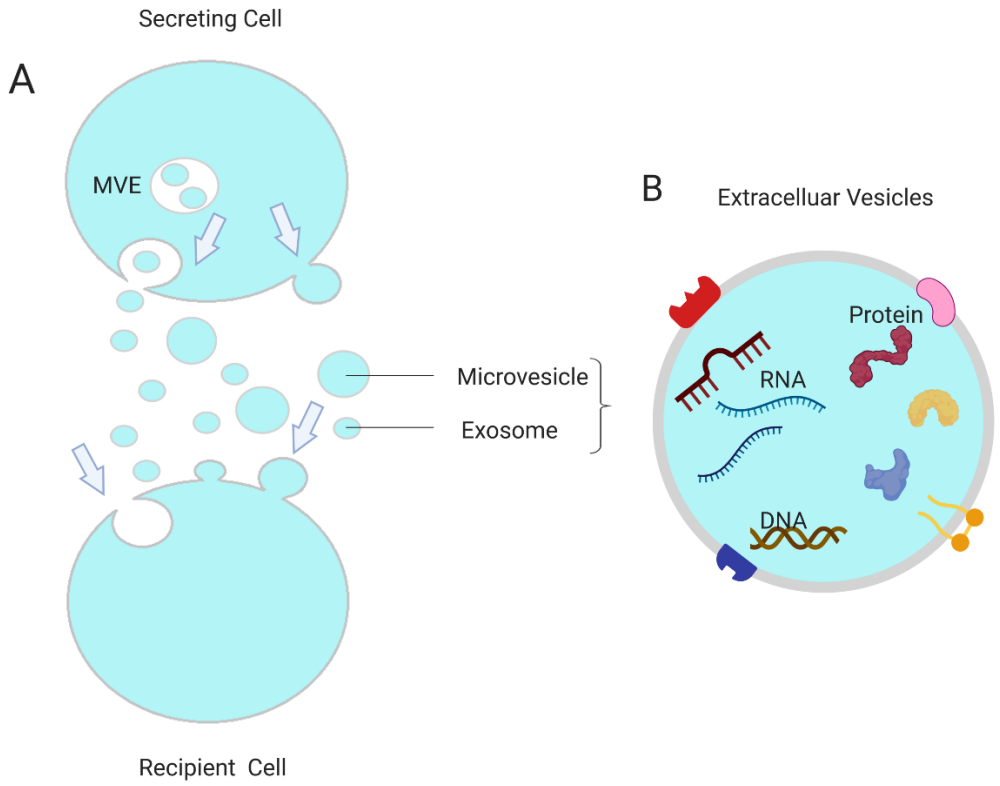

Figure 1.1 Schematic representation of cell to cell communication of EVs (A) and inner content of EVs (B).

Cellular communication is an important strategy to maintain tissue and systemic homeostasis. A typical pathway for intercellular communication is mediated by a “release-capture” pattern for EVs between

parental cells (**Figure 1.1**). In extracellular space, EVs originating from the parental cells and delivered to the target cells, shuttle signalling molecules thus protected them from degradation. [6-11] EVs are proved to be not only transferred to neighbouring cells but can also travel to other areas in the body. Moreover, EVs are not only released during normal physiological conditions, likely reflecting the physiological conditions of the cell but also revealing the stress condition. In this context, they regulate the immune responses, [12-14] in inflammation reactions, [15-17] and tissue regeneration.[18, 19] EVs have also been associated with pathological conditions including cancer [20-23] and neurodegenerative diseases,[24-26] where the secreted amounts have been reported to increase with specific disease states. [23-27] The features mentioned above make the EVs as a promising topic in further biomedical research.

1.1.2 Diagnostic and therapeutic potential

In recent days, EVs triggers a rapidly increasing interest in the field of biomedical research, due to their several applications in diagnostics and therapeutics.[28-33] As an emerging biological role in the diagnostic area, EVs with various bio-content reflect many pathophysiological states of the body, such as pregnancy, ageing, and disease. For instance, specific biomarkers may reflect certain pathology inside the body. Most studies on biomarkers from urinary EV are linked to kidney diseases,[34, 35] and cancers, [36] mostly of the urogenital system such as bladder,[37, 38] and prostate cancer.[38, 39] There also have been attempts to find urinary biomarkers for other disorders, including brain diseases[40] and bladder dysfunction. [41] Therefore, it would be ideal for the diagnosis and monitoring of patients with upper and lower urinary tract diseases. For example, Pocsfalvi et al. conducted pioneering investigations to determine whether changes in the protein content of EVs occur during the progression of autosomal dominant polycystic kidney disease (ADPKD), a common genetic disorder that predominantly affects the kidneys. [2] Circulating tumour-derived EVs actively participate in tumour initiation progression and metastasis. Recently, methods have been developed to isolate tumour-derived EVs by capturing candidate tumour-regulated markers on the EV membrane.[42-45] Even biomarkers that distinguish tumour-derived EVs from normal EVs have not been completely revealed yet, expectations on EVs-related technologies in the field of cancer diagnostic and treatment are enormous.

Another highlight and advantages of the EV based diagnostic methods are less invasive as well as less complexity. To determine the diseases related biomarkers from the patient, tissue biopsy collection was used as the ideal standard method for the diagnosis and monitoring of many urological disorders and various diseases. However, it is an invasive procedure with limited reproducibility, which could exhibit the high variability between the biopsy samples from the sample source is a significant drawback.[46] Moreover, it is difficult for the small sample size of tissue biopsy to provide detailed information about genetic heterogeneity within the primary tumour or metastasized secondary tumours. As an alternative, body fluid such as urine may consider as an ideal diagnostic source since it is easy to collect non-invasively. In clinical diagnostics, urine is one of the commonly used body fluids, which is biomarker-enriched and could routinely be collected to diagnose and monitor several diseases. However, most studies utilize total, unfractionated urine samples, comprised of a complex mixture of salts, proteins, metabolites, cells, and cell debris, which mostly originate from the upper and lower urinary tract or filtered directly from the systemic circulation, which could pose challenges for biomarker detection.[46, 47] In this case, EVs-based "liquid biopsy" merits consideration over conventional tissue biopsy for several reasons. It provides a convenient and minimally invasive way of diagnosis over tissue biopsy that requires surgery. The unique biomolecules packaged within EVs and the surface biomarkers provide the starting material for the EVs based diagnosis. Certain biomarkers are also encapsulated in the lipid membrane against degradation in an environment with high nuclease content during urine passage. This makes EVs a promising diagnostic biomarker for various health disorders, both in the early and ongoing stages of disease progression.

In therapeutic application, the ability of EVs to be taken up by a large variety of cells has directed investigations towards the use of EVs, or mimetics,[48, 49] as cargo carriers in drug,[50, 51] or RNA and vaccine delivery applications.[52-55] In the discipline of drug-carrier design, to qualify as competent drug delivery carriers, EVs should be capable of loading a substantial amount of therapeutic cargo and specifically transfer into the target cells or tissue. A variety of cargos, e.g. small interfering RNA (siRNA), miRNA, and other therapeutic compounds such as drugs, have now been shown to exhibit a strong therapeutic effect after EV-based delivery to particular tissues. Methods for loading EVs with substantial amounts above mentioned therapeutic cargos have been studying to achieve a successful delivery. The current approach of therapeutic loading content to EV includes the traditional method such as electroporation,[56, 57] simple incubation with cargo,[58, 59] sophisticated methods like transfection or activation of the exosome donor cell. Another essential requirement for EV-targeted therapy is the targeting peptide or protein must be present on the surface of those drug delivery vehicles. This could be used as a superiority to increase the accuracy and efficacy of EV-based drug delivery to pathological tissues, especially in cancer treatment, where chemotherapeutics might impose negative side effects on other tissues. The technique aims to optimize and ensure a successful insertion of the target peptide to EVs. For example, studies found that usage of RVG and iRGD as targeting peptides on a Lamp2b pedestal significantly increased the specificity of the treatment, and also enhanced the cellular uptake of the exosomes in the tissue of interest.[60, 61] After all, several completed and ongoing diagnostic and therapeutic clinical trials are described, indicating that EVs or exosomes based diagnostic system and drug delivery systems may have advantages in a variety of application. However, due to the endogenous origin, their design and application need to be refined and verified to maximize their further usage on the large clinical scale.

From the above literature evidence and discussion, it was found that EVs has tremendous application in both diagnostics and therapeutics. Therefore, to make the widespread use of EVs applications to clinical trials, accurate quantification of EVs is inevitable.

1.2 Quantification of EVs

EVs are increasingly recognized as important diagnostic and therapeutically entities. Therefore, accurate quantitative analysis of EVs and its contents has always been considered as an essential and challenging topic.[62, 63] However, standardized methods for their analysis are still lacking. The establishment of such methods is crucial for the safe application of engineered EVs in clinical practice, but EV quantification has proven technically challenging due to their small size and their heterogeneity in size and composition. Generally, the current quantification method for EVs is classified into two categories. First, the quantification method usually refers to quantify total biomolecular content (protein, RNA, lipid)[64, 65] or counting the number of vesicles carrying particular EV biomarkers such as surface proteins or inner miRNA,[66, 67] while the second method suggests counting particles by their physical properties, e.g. size .[68, 69]

1.2.1 Quantification by total molecular content

In the previous study, EVs concentration usually refers to the total protein concentration in EV-enriched samples determined by the classical protein quantification method.[70] This technique usually relies on the known individual protein extinction coefficient or a standard. However, precise quantification of the total protein concentration is difficult owing to the heterogeneity of proteins and their unknown extinction coefficient in EV samples. In this context, building a calibration curve of protein solution with a known concentration and determine the total protein content bind to coloured reagent by colorimetric assays could provide a decent result of total protein concentration. The commonly used method includes colorimetric assays such as bicinchoninic acid assay (BCA assay) due to its convenience, high sensitivity.[71, 72] Moreover, with better compatibility with detergents, BCA assay is exceptionally competent to quantify the real total protein content; it includes not only the proteins exposed to the lipid membrane, but also encapsulated protein while the EVs are treated with a lysing reagent.[73, 74]

In comparison with proteins, the determination of other biomolecular content from EV such as RNA or lipid is not the common use method to quantify EVs. Even some techniques, including UV–VIS spectrophotometry and fluorometry using fluorescent dyes specific to nucleic acid material are capable of determining the concentration of RNA in vesicle samples by Bioanalyzer, Nanodrop, and qRT-PCR techniques.[75-77] Instead, the quantification of RNA, as well as lipid, has been regarded as a standard of EV purity by related to the concentrations of proteins in EV samples.[75, 78]

One of the main limitations of the above-mentioned methods is that the quantification results are largely fluctuated by the purity of EV samples, making the isolation method directly influence the EV's quantification. Any non-EV content can contaminate the sample and affect the measuring data. As a result, the purification during the EV sample is significant to eliminate the contamination with minimum EV loss. On the other hand, an increase of the protein concentration in EV samples, for instance, could refer to either more concentrated EV particles or an increase of protein content per vesicle or even both. Hence, it is suggested that the total biomolecule quantification data should ideally be complemented with particle counting based on their physical properties, which will be discussed in the next section.

Another quantification method of vesicles presents within complex suspensions is based on specific biomarkers. This can be achieved by techniques that provide a count of particles either have specific surface protein or carrying certain RNA inside their membrane. With the help of specific antibodies or molecular probes,[79, 80] specific sets of vesicles can be selected by targeting different types of membrane proteins such as disease biomarkers (CD9, CD63 and CD81), markers for a specific subpopulation of EVs, or cell/tissue-specific markers to determine the vesicle origins. It has been shown that EVs are enriched in several groups of proteins such as tetraspanins, heat shock proteins, Rab proteins, lipid raft-associated proteins and proteins taking part in the formation of multi-vesicular bodies.[81, 82] Nevertheless, the progress of the EV field may lead to establishing specific markers for EV subpopulations, which

could then potentially be used to quantify several subsets of vesicles in a sample. Currently, quantification of a specific subset of EVs based on their membrane marker using immuno-recognition approaches can be carried out either by taking advantage of a solid surface-functionalized with one of the binding partners, including enzyme-linked immunosorbent assay (ELISA), surface plasmon resonance (SPR), etc. On the other hand, fluorescent flow cytometry and fluorescence-based NTA are exhibiting a promising application is this field based on solution-based quantification. For the biomarker-based method, one of the drawbacks is antibodies as well probes used to proven biomarkers and EV standards are required, which is relatively costly.[83-86]

1.2.2 Quantification by physical properties

Nowadays, the EVs quantification depends upon the detection of individual particles based on their physical properties. To accurately quantify EVs in terms of their total particle numbers, their properties such as morphology, size, optical properties, density and charge are essential. One of the most common uses of physical characterizations of small EVs is based on their size, which has been facilitated by the development of a number of methods allowing for the detection of objects with characteristic sizes below 200 nm. Transmission electron microscopy (TEM) has been widely utilized for EVs based on their structure and morphology. However, extra precaution should be taken while using these methods because the procedures significantly damage the fragile vesicles and affect their size and morphology, ultimately affects the result.[87, 88] Furthermore, Nanoparticle tracking analysis (NTA) is the most commonly used technique for EVs, which allows the direct visualization of individual scattering particles illuminated by a laser beam. The hydrodynamic radius of a single particle is determined after tracking its Brownian motion. Since the particles can be directly visualized, NTA can also be used to determine the size distribution as well as quantify the number of particles in solution. Over the last years, NTA as a fast and convenient sizing technique has been widely employed in EVs quantification.[89-93] However, NTA is a label-free technique where vesicles present in complex biological suspensions may be challenging to distinguish from other types of particles and, in particular, from protein aggregates.[94, 95] Furthermore, considering the small size typically below the diffraction limit of visible light, small EVs cannot be resolved by standard optical microscopy. Like NTA, other methods, including dynamic light scattering (DLS), are also capable of determining the size distribution level, which can directly provide the concentrations EVs (particles/mL).[3, 4] Several commonly used methods for EVs characterization and quantification are summarized in **Table 1.1**

Table 1.1 Commonly used methods for the characterization and quantification of EVs.

Principle of EVs Analysis	Property	Analytical Methods used
Physical	Structure and Morphology	TEM,[89-93] AFM [96-98]
Physical	Size	DLS,[99-101] NTA, [89-93] tRPS [102-104]
Physical	Zeta Potential	RPS,[105] Micro-CE [106]
Biochemical	Total protein	BCA Assay [71, 72]
Biochemical	Total RNA	Bioanalyzer, Nanodrop, qRT-PCR [75-77]
Biochemical	Total Lipid	Sulfophosphovanilin assay [107]
Biochemical	Specific RNA	Exochip [108]
Biochemical	Specific Surface Protein	ELISA,[67, 109] SPR,[110, 111] Flow cytometry [112, 113]

In my study, EVs are quantified by the capillary electrophoresis, concerning their total RNA content. However, flow cytometry is required in the set-up of this quantification method in order to calculate the

average mass of RNA in each EV particle.

1.3 Capillary electrophoresis

Electrophoresis is an electrokinetic phenomenon where the motion of charged species/particles relatively to a medium fluid under a uniformed electric field. In an electrolytic cell, positively charged particles (cations) move to the cathode, and negatively charged particles (anions) move to an anode. There are several well-known applications of electrophoresis, such as nucleic acid, protein gel electrophoresis, and Western blot. Nowadays, electrokinetic separation is not limited to "gel stations" and can be performed in small nano- to micrometre channels; this technique was named capillary electrophoresis (CE).[114]

There are several modes of CE. The most widely used technique is capillary zone electrophoresis (CZE), which is a conventional CE mode in a blank buffer. To analyze the diluted samples, capillary isotachophoresis (CITP), which preconcentrates analytes first, can be used. Another technique is capillary isoelectric focusing (CIEF), which utilizes a pH gradient to separate analytes according to their isoelectric point and is usually applied to separate the protein. In-gel CE (GCE), a separation capillary is filled with a modified buffer containing dissolved polymers or a gel; this approach was previously widely used for nucleic acid sequencing. Non-ionic analytes can be separated in CE with the help of liposomes, micelles or emulsions. These techniques are called liposome electrokinetic chromatography (LEKC), micellar electrokinetic chromatography (MEKC), and microemulsion electrokinetic chromatography (MEEKC), respectively.[115] Affinity CE (ACE) is used to separate analytes that have different affinities to a target molecule added to the separation buffer.[116] In my work, I utilized CZE.

Capillary electrophoresis is an analytical method consist of a setup (**Figure 1.1**) consists of a fused silica capillary (inner diameter 10-100 μM, outer diameter 150-400 μM) as a separate channel, a direct high-voltage current (usually 5-30 kV) electric field as a driving force, two buffer reservoirs for inlet and outlet ends of the capillary and a detector (often photodiode array (PDA), UV absorption (UV) or laser-induced fluorescence (LIF)).

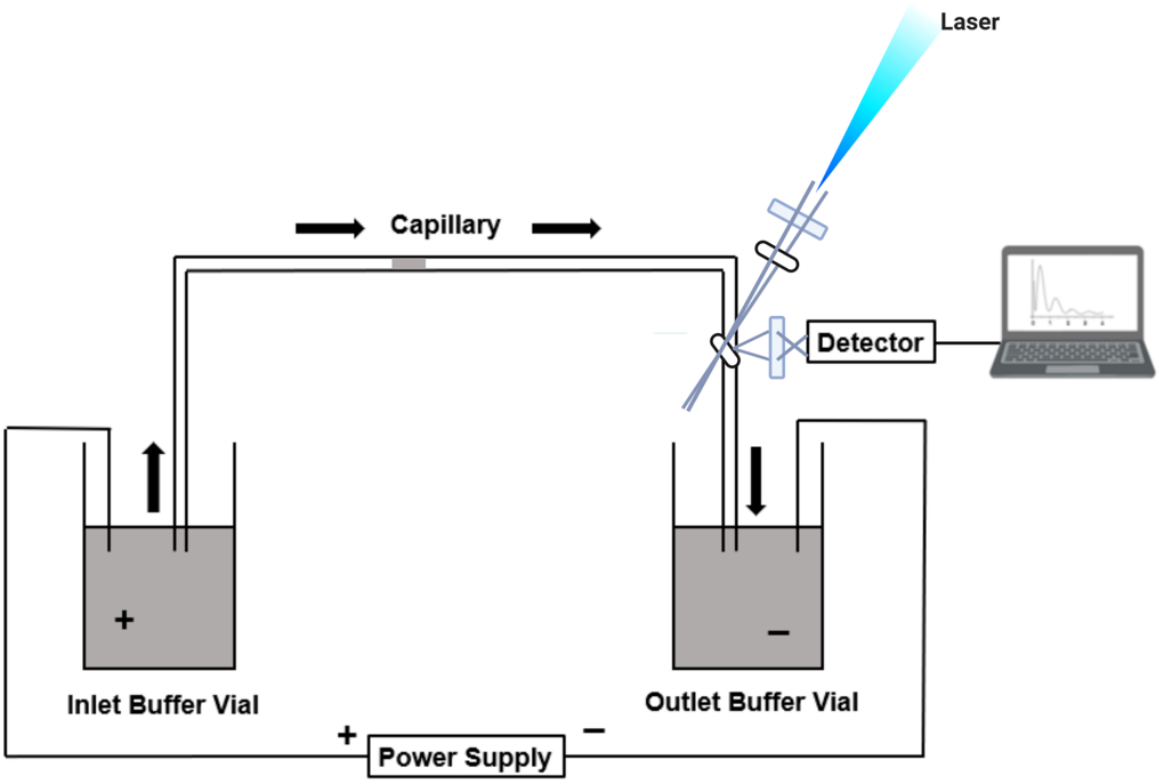

Figure 1.2 Schematic representation of a basic capillary electrophoresis setup.

The separation is achieved based on the difference in the mobility of each component (migration speed under unit electric field strength) or the distribution behaviour. When the fused silica capillary is filled with the operating buffer, the silanol groups (SiOH) on the inner wall of the tube dissociate and release hydrogen ions (H^+) into the solution, making the wall negatively charged and forming an electric double layer (ζ potential) with the solution. This layer is the first layer of the system, which is semi-permanently attached, followed by the second layer of ions, which is mobile and able to migrate.

When a DC voltage supply is applied to the two ends of the capillary tube, the positively charged ions in the second layer begin to move towards the cathode terminal with their drag of the solution as a whole. This overall movement of the solution under the electric field is called electroosmotic flow (EOF). The schematics of the EOF are depicted in **Figure 1.2**.

The degree of dissociation of the inner silanol groups is related to the pH of the operating buffer and the modifiers added. Decreasing the pH of the solution will reduce the dissociation degree and reduce the electroosmotic flow; increasing the pH of the solution will increase the dissociation degree and increase the electroosmotic flow. This bulk flow has a uniformed profile in the capillary as opposed to a laminar flow created by the pressure differential (**Figure 1.3**).

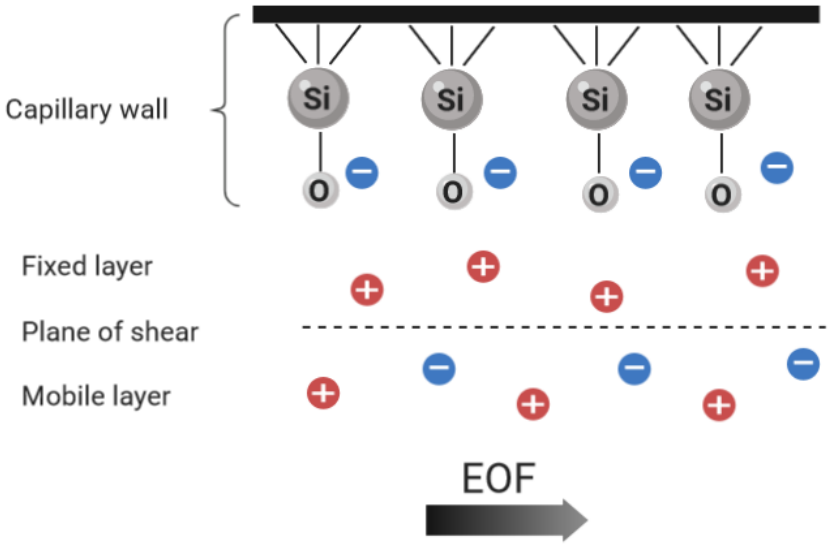

Figure 1.3 Schematic representation of electroosmotic flow (EOF) in a capillary. Si-O- represents a fixed layer; positively charged particles next to it represent a mobile layer, which creates a bulk flow of liquid.

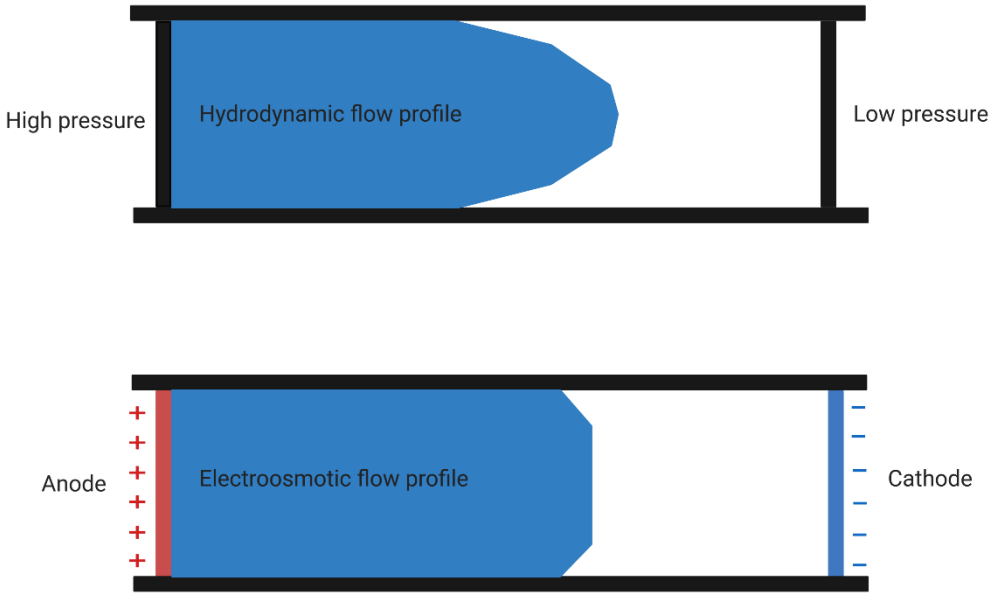

Figure 1.4 Difference in flow profiles between pressure-assisted laminar flow (an upper capillary) and EOF (a lower capillary).

EOF depends on silanol deprotonation and is suppressed at pH's around 2-3 and increases with increasing pH. The ionic strength of a separation buffer can also influence EOF due to the fact that high

concentrations of ions decrease zeta potential (ζ), as in equation 1.1:

$$V_{EOF} = (\varepsilon\zeta/\eta)/E \quad (1.1)$$

Where V_{EOF} is the velocity of EOF, ε is dielectric constant, and E is an applied electric field.

In electrophoresis, ions are separated based on their velocity (V), as in equation 1.2:

$$V = \mu_e E \quad (1.2)$$

Where μ_e is electrophoretic mobility, α is the degree of ionization (or dissociation) of a molecule, E is applied electric field. The mobility is determined by the ratio of electric force and drag force exerted on the particle, as in equation 1.3:

$$\mu_e a = \frac{F_E}{F_F} \quad (1.3)$$

The electric force is proportional to ion's charge (q), as in equation 1.4:

$$F_E = qE \quad (1.4)$$

The frictional force for the spherical ion is proportional to its radius (r), ion velocity (V) and solution viscosity (η), as in equation 1.5:

$$F_F = -6\pi\eta r V \quad (1.5)$$

From these equations, it can be concluded that in electrophoresis, the slowest ions are bulky slightly charged, and the fastest ions are small and highly charged.

The electroosmotic velocity is usually greater than the electrophoretic velocity when the pH is above 4. Therefore, even anions will flow from the anode end of the capillary to the cathode end during electrophoresis. Smaller and more highly charged is an anion easier it is for it to resist EOF, moving slower, and smaller and more highly charged is action stronger it outstrips EOF, moving faster (**Figure 1.5**).

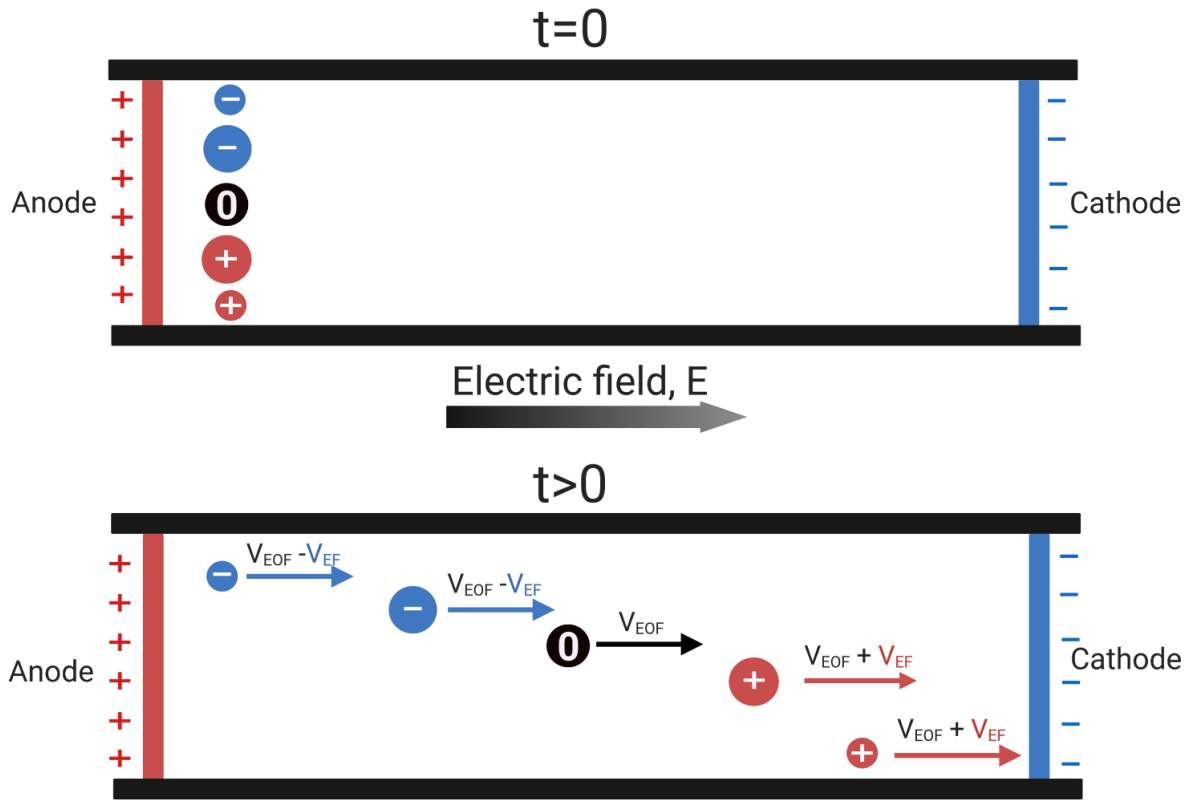

Figure 1.5 Schematic representations of analytes movement in CE base on their charge and size.

1.4 Research objective

Accurate quantitative analysis of EVs and its contents has always been considered as an essential topic. Literature evidence suggests that several approaches have been proposed to determine the concentration of EVs, which are based either on the counting of particles by physical properties or the quantification of biomolecules. However, those quantification methods of EVs and substantially differs from each other with their limitations, and there is currently no gold standard method of quantification for such particles. In this study, a new method of EV quantification has been demonstrated for efficiency, speed, and quality control of extracellular vesicles by capillary electrophoresis. This quantification method is demonstrated for EVs from two sources (i) EV isolated from three cancer cell lines. (ii) EVs isolated from urine samples from healthy individuals.

The first part of this thesis illustrated the isolation and characterization of EVs from three cancer cell lines, as well as human urine samples. Differential ultracentrifugation was performed to obtain EVs, followed by the analysis by TEM, NTA and flow cytometry for obtaining the information of harvested EVs.

In the second part of this thesis, inspired by the previous work of our research group on Viral quantitative Capillary Electrophoresis (Viral qCE),[117, 118] I focused on using capillary electrophoresis for EVs quantitation (EVqCE). In this study, I performed capillary zone electrophoresis with laser-induced fluorescent detection to separate intact EVs from DNA and RNA impurities. YOYO-1 dye was used to stain all DNA and RNA in the sample, including the free one and encapsulated one. After lysis of EVs with a detergent, encapsulated DNA and RNA were released. After additional RNase

treatment of the EVs sample, RNA was enzymatically cleaved, leaving residual DNA only. A calibration curve of RNA for cancer cell lines EVs and a standard addition plot of RNA for urine EVs were made by the same CE instrument to quantify RNA released by EV lysis. Meanwhile, flow cytometry was performed to quantify EVs stained with YOYO-1 and FM 5-95, to figure out the amount of lysis EVs. Combined CE results and the data obtained from flow cytometry, the average weight of RNA in each EVs defined as$[M_{RNA}]$, was calculated (g/particle). EVqCE worked in a dynamic range of EVs concentrations from 10^8 to 10^{10} particles/mL. Once the value of$[M_{RNA}]$ is obtained, the following process can be completed in less than one hour and requires minimum optimization of CE separation.

Lastly, to apply EVqCE to EVs quality control, the degree of EVs degradation after sonication, vortexing, freeze-thaw cycles and storage was examined. Different levels of degradation were observed after processing, suggested the ideal possibility of real-time monitoring of EVs and the quantification content, which would lead to excellent application prospects in future EVs research and rapid quality testing in pharmaceuticals.

Chapter 2. Isolation and Characterization of Extracellular Vesicles

2.1 Objective

The EVs were enriched from cancer cells as well as urine collected from healthy individuals by the ultracentrifugation process. Based on the morphology, size and surface markers, different analytical techniques such as TEM, NTA and flow cytometry were utilized to confirm the presence of EVs in the sample.

2.2 Materials and methods

2.2.1 Chemicals and Materials

The following chemicals were purchased: The anti-Human CD9 PE, (Cat# 353008); Anti-Human CD63 APC, (Cat# S32703) were used to characterize the EVs in flow cytometry. The cancer cell lines: breast cancer (MDA-MB-231), lung adenocarcinoma cell line (NCI-H1975) and T lymphoblast cell lines (CCL-119) were purchased from ATCC (U.S.A). Dulbecco's phosphate-buffered saline (Cat.no. D8537, Sigma, U.K), Dulbecco's modified eagle's medium-high glucose (Cat.no. D5796, Sigma, U.K), RPMI-1640 medium (Cat.no. R8758, Sigma, U.K), fetal bovine serum (Cat.no.17D192, Sigma, U.K), antibiotic (Cat.no.15140-122, Gibco, U.S.A) was used in the following experiments.

Dulbecco's Phosphate Buffered Saline, Dulbecco's Modified Eagle's Medium-high glucose, RPMI-1640 Medium, Fetal Bovine Serum (FBS) were purchased from Gibco by Life Technologies. In order to remove internal EVs, FBS was centrifuged at 100,000g; the supernatant was collected. The antibiotic solution was purchased from Gibco, USA. All the buffers were made using Milli-Q-quality deionized water and filtered through a 0.22 µm filter and stored at 4℃ for further use.

Preparation of EVs free medium: EVs are present in the serum (FBS), which is generally used for routine cell culture. To avoid contamination by these EVs, the culture medium used to grow cells must be depleted of EVs. For this, 50 mL of FBS was ultracentrifuge at 100,000 g for 17 h using the SW28 swinging bucket rotor (Beckman Coulter, USA). After centrifugation, the supernatants were collected slowly into a separate tube and stored at 4°C for further use. To prepare EVs free medium, i.e., the complete media, 10% of EVs free FBS and 2-3% antibiotics were added and stored at 4°C for further use.

2.2.2 EVs collection

MDA-MB-231 cells were grown in DMEM medium, while both NCI-H1975 cells and CCL-119 cells were cultured in RPMI-1640 medium, at 37 °C in 5% CO_2/air. Above mentioned mediums were supplemented with 10% EVs-depleted FBS and 1% of penicillin and streptomycin antibiotics. MDA-MB-231, NCI-H1975 and CCL-119 cells were cultured individually from 48 h to 72 h or up to 70-80% confluency in EV-depleted media before the harvest of EVs. The early morning urine sample was collected from healthy volunteers (n = 3; 2 male, 1 female; age range 21−25 years) and transferred into falcon tubes (50 mL). The urine sample collection was performed according to the ethics approval from the University of Ottawa (Ethics File no: H-08-18-980, Certificate attached in supplementary file). Each sample was supplemented with 1mM $ZnSO_4$ (Sigma, USA) and incubated at 4˚C for 12 h in order to remove protein contamination, e.g., uromodulin and Tamm-Horsfall glycoprotein. The removal will prevent the formation of extracellular filaments, which is likely to co-sediment with EVs.

The method of EVs collection from urine and cancer cells are mostly similar. The procedure involved a number of centrifugations, which sequentially increased the speed and time, and thus pellet the smaller particles. The pellet was discarded from each run, and subsequent centrifugation was performed on the supernatant from the previous sample until the last centrifugation, which pelleted the EVs. To harvest EVs from cancer cells and urine, urine samples, as well as conditioned medium harvested from cultured

cells, were centrifuged at 300 g for 10 min to remove cell debris and large protein complex. The pellet was discarded, then the supernatant was collected, followed by centrifuged with 2000 g for 30 min to remove apoptotic bodies. The pellet was discarded, and the supernatant was further subjected to ultracentrifugation at 100,000 g for 3 h at 4˚C in an ultracentrifuge using the SW28 Ti rotor (Beckman Coulter, USA). The schematics of EVs isolation and enrichment procedure for cancer cell lines and the human urine samples are presented in **Figure 2.1** and **Figure 2.2,** respectively.

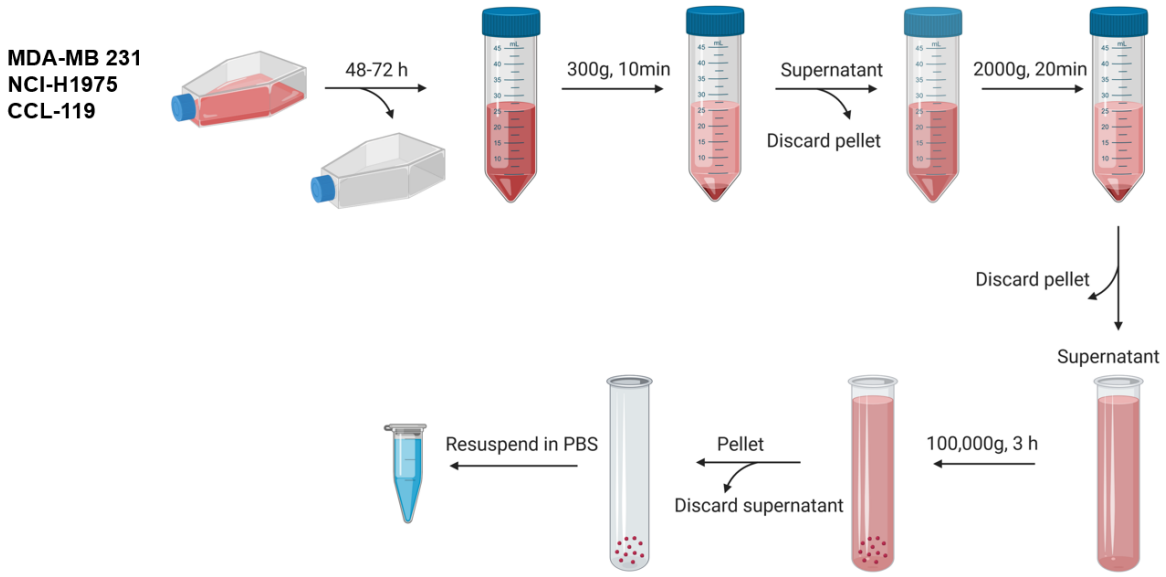

Figure 2.1 Schematic representations of the isolation of EVs from cancer cells.

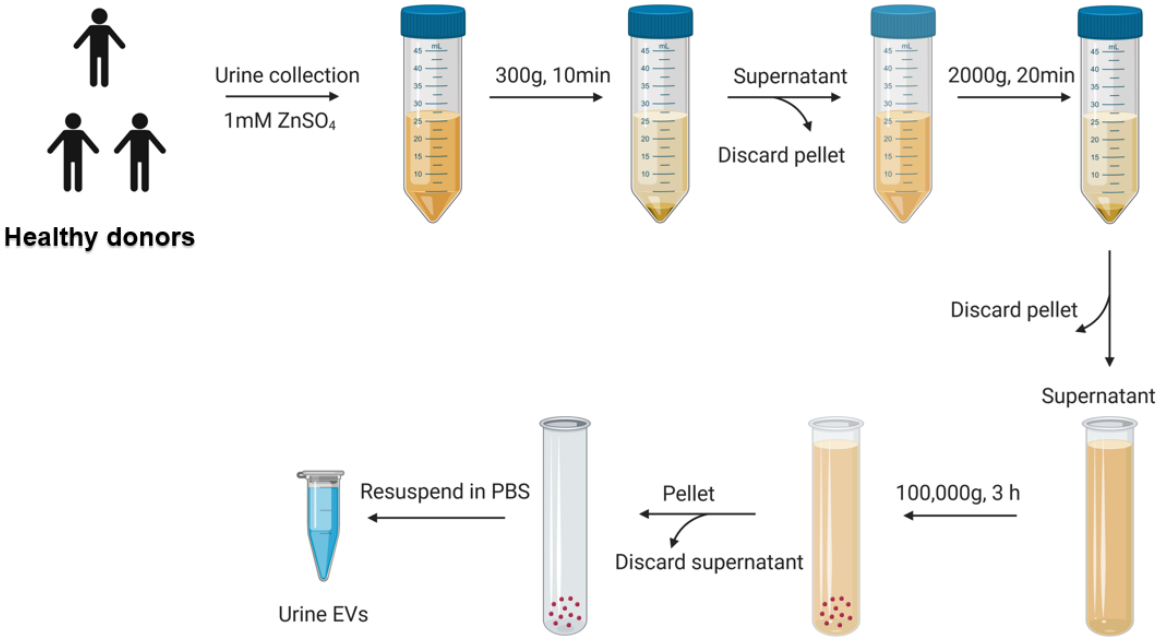

Figure 2.2 Schematic representations of isolation of EVs from the urine sample.

2.2.3 Transmission Electron Microscopy (TEM)

Formvar® coated copper grids (200 mesh; Canemco, Lakefield, ON, Canada) were glowed charged for 45 seconds. EVs suspensions (10µl) were spotted on grids for 5 mins. After removal, samples were negatively stained with 2 % UranyLess (Cat # 22409) in water for 1 minute and dried with filter paper. Subsequent air dry for 30 mins, EVs were examined on a transmission electron microscope (JEOL JEM 1230, Japan) operated at 50 kV. The Feret's diameter of the particles was analyzed using ImageJ software.

2.2.4 Nanoparticle tracking analysis (NTA)

The ZetaView nanoparticle tracking microscope PMX-110 (Particle Metrix, Germany) was used to characterize the harvested EVs. The particle concentrations and size distribution confirmed the presence of EVs isolated from the cell culture conditioned media as well as a urine sample. Polystyrene beads of 102 nm in size (Microtrac 900383) were used as an external control before each experiment. The EVs were diluted in 1X PBS to achieve a concentration within the $10^5 – 10^7$ particles/mL range for optimal analysis.

2.2.5 Flow cytometry

Beckman Coulter MoFlo Astrios EQ was adapted and optimized to nanoscale particle detection. The buffers were filtered by 3 kDa (Amicon® Ultra-15 Centrifugal Filter Units) before using to reduce backgrounds. The buffers with antibodies and dyes were analyzed as controls for background counts.

For the validation of selected EVs, isolated exosomes were subsequently incubated in the dark for 20 min with two antibodies, i.e. anti-human CD9 PE and anti-human CD63 APC. The control samples included the unstained EVs and pure buffer samples. The data from flow cytometry were analyzed using the Kaluza analysis software.

2.3 Result and discussion

2.3.1 EVs collection

Differential centrifugation separation is mainly based on the size of different particles. This isolation technique has been used widely for the isolation of EVs and is considered as the "gold standard" method for EVs isolation. In my study, differential centrifugation was applied to cancer cell line media as well as urine. The final yield of EVs from cancer cell lines may vary by culturing time before collection, while the amount of urinary EVs from did not show a significant difference between three volunteers.

2.3.2 Characterization of EV by TEM

In this study, TEM was utilized to capture the images of EVs from cancer cells and urine samples, which is capable of confirming the presence of EVs with direct visualization. The image depicted that the isolated vesicles were round with relative sizes ranging from 30-200 nm. Also, the images show that there was some contamination with cellular debris showed a dark colour (**Figure 2.3**).

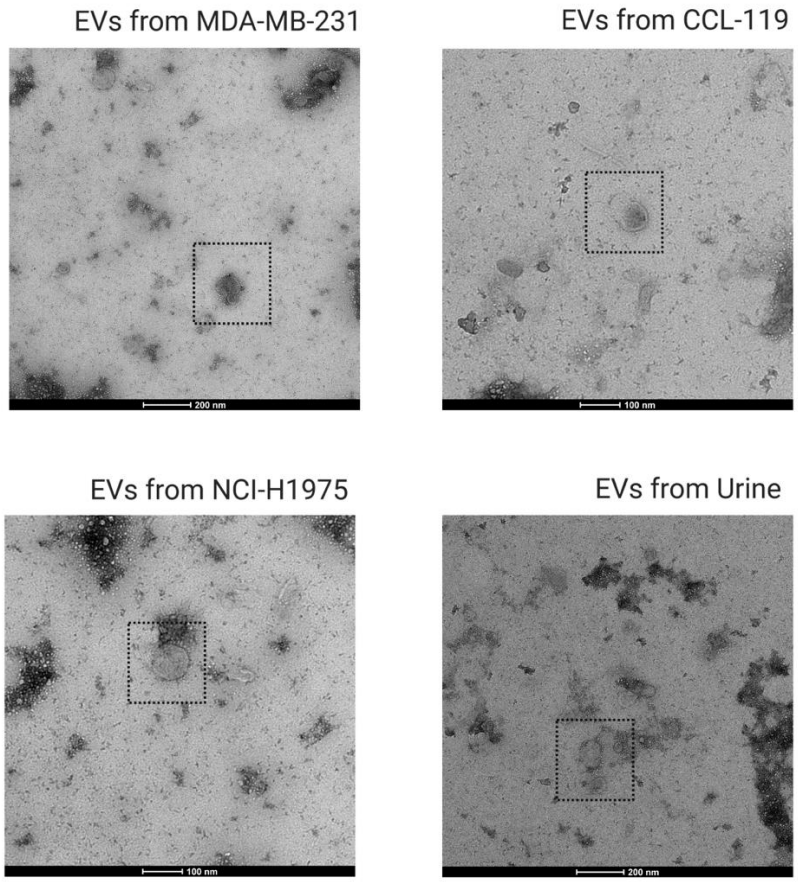

Figure 2.3. Transmission Electron Microscopy (TEM). TEM images of EVs derived from human urine and different cancer cells, including MDA-MB231, NCI-H1975, CCL-119. EVs samples were negatively stained with 2% UranyLess after removing the extra moisture. Sphere-shape structures, with a size around 100 nm and visible membrane, were identified as being EVs particles (confined in dot shape).

2.3.3 Analysis of EVs by NTA

NTA provides counts and sizes of particles by measuring their Brownian motion in solution. In my study, NTA was applied to quantify the EVs isolated from urine samples as well as cancer cell lines with a range of size and their concentrations. The size distributions of EVs from MDA-MB-231, NCI-H1975, CCL-119 cells and urine are presented in **Figure 2.4.** The peak diameter is 105.8 nm, 136.2 nm, 174.3 nm and 123.6 nm, respectively. The concentrations of the EVs was found to be 2.3×10^9 particle/mL, 4.4×10^9 particle/mL, 2.6×10^9 particle/mL and 1.3×10^{10} particle/L. This value of EVs from urine is relatively higher, partially caused by the existence of impurities like protein aggregates.

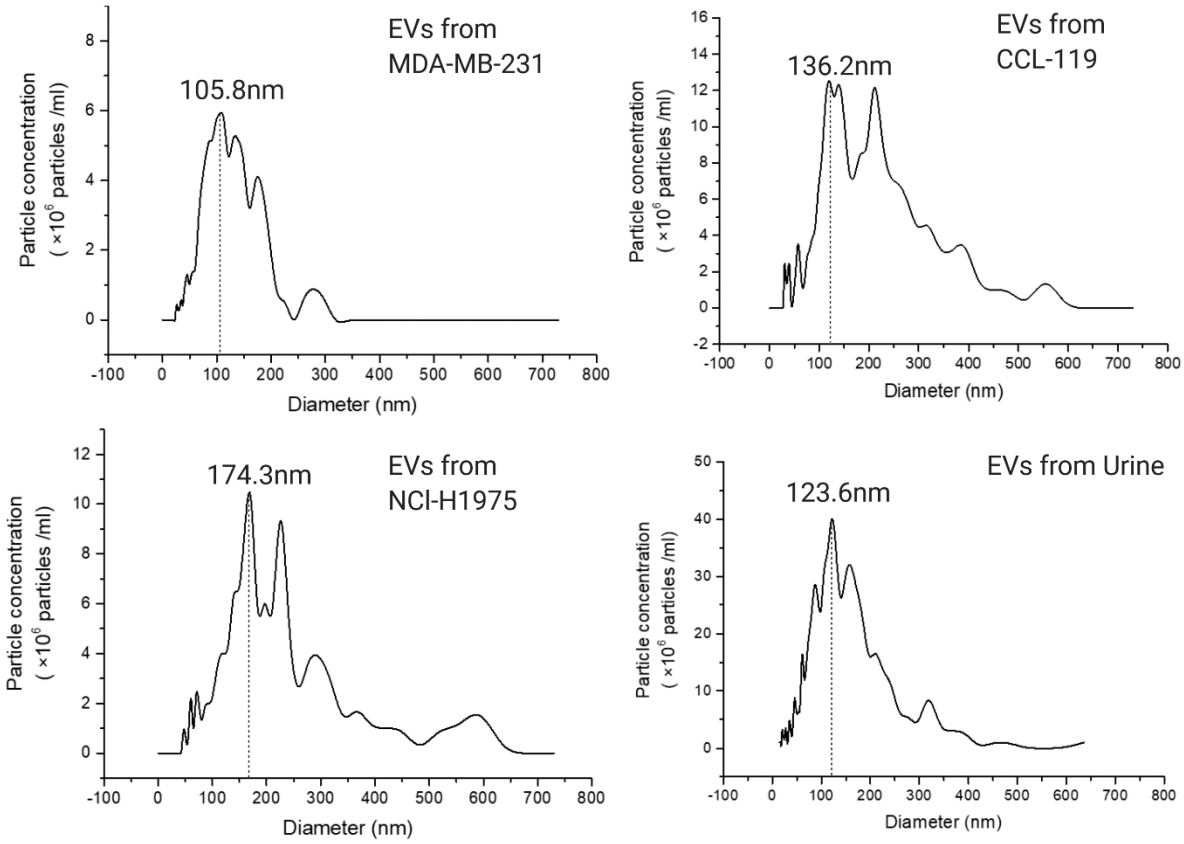

Figure 2.4. Nanoparticle tracking analysis (NTA). The size distribution of EVs derived from human urine and different cancer cell lines, including MDA-MB-231, NCl-H1975, CCL-119. The maximum peak diameter of the respective EVs has been depicted with the dotted line.

2.3.4 Analysis of EVs by Flow cytometry

CD63 antigen is a protein that is encoded by the CD63 gene. CD9 is a gene encoding a protein that is a member of the transmembrane four superfamilies, also known as the tetraspanin family. Both of those antigens commonly exist on the surface of EVs, which are regarded as biomarkers for the confirmation of EVs.[119] In our experiment, anti-CD63 APC antibody and anti-CD9 PE antibody were used to mark the positive subpopulation of EVs to present the existence as well as the concentration of EVs. 20-45% of those vesicles have represented a population of both antibodies labelling. This result confirmed the presence of EVs in the sample after the harvest process.

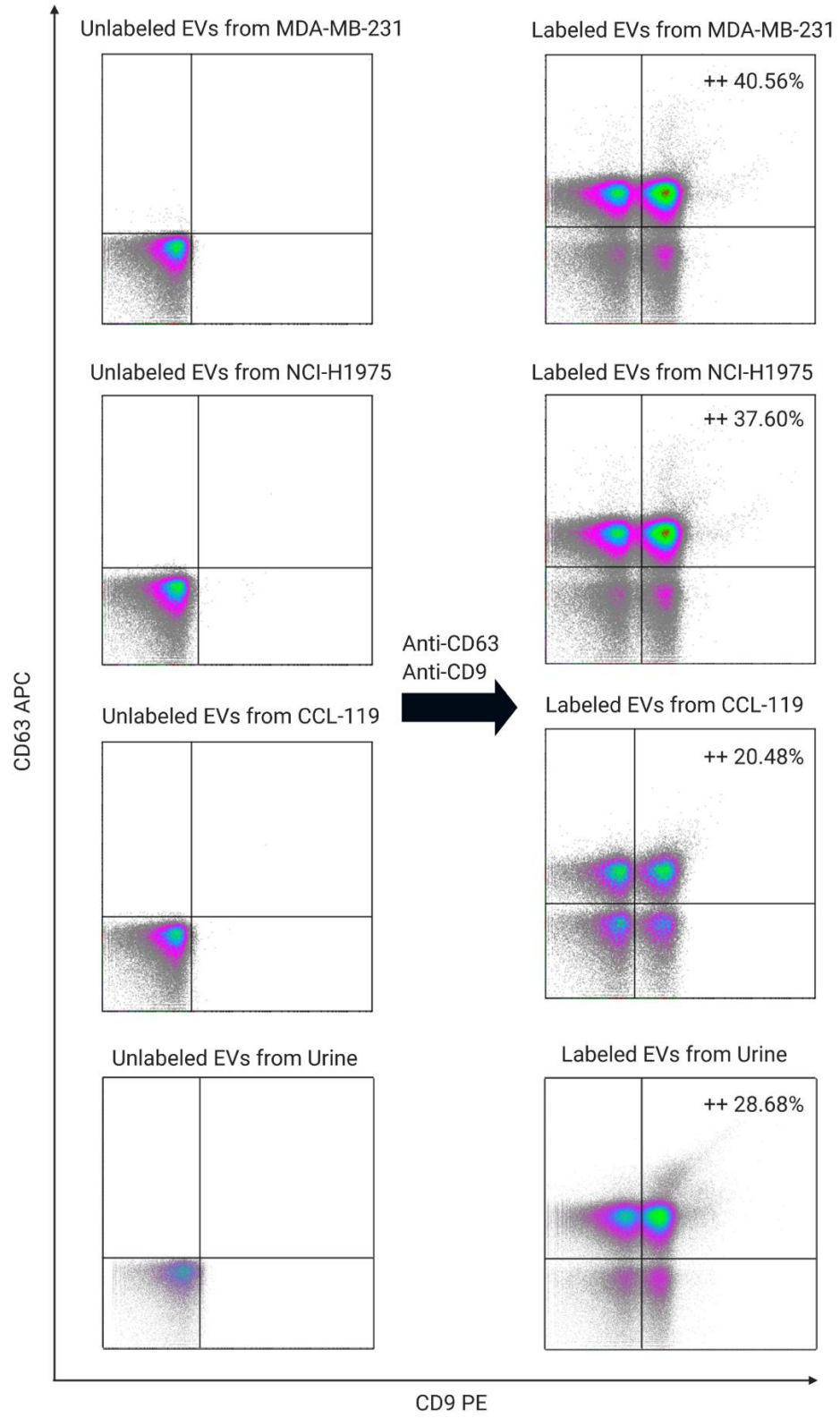

Figure 2.5 Flow cytometry analysis EVs derived from human urine and different cancer cells, including MDA-MB-231, NCl-H1975, CCL-119, stain with Anti-CD63 APC Antibody and Anti-CD9 PE Antibody.

2.4 Conclusion

The result from TEM, NTA and flow cytometry confirmed that the harvested particles had the hollow membrane-based structure, with CD-9 and CD-63 antigens (surface markers) and the size of 100 -300 nm. These features meet the common standard of EVs in other studies.[120] Also, the concentration of EVs was found to be from 1×10^{9} particles/L to 1×10^{10} particles/mL, indicating enough particles for further studies.

Chapter 3. Quantitative Capillary Electrophoresis for Extracellular Vesicles

3.1 Objective

A quick and accurate quantitative analysis of EVs and their contents has always been considered an essential topic. Herein, I introduced the EVqCE as a method to quantify EVs from unknown EV-enriched samples.

3.2 General procedure

3.2.1 Chemicals and Materials

The following chemicals were purchased: sodium borate decahydrate (cat# SX0355-1, EMD Chemicals, U.S.A); YOYO-1 Iodide (cat# N7565, Invitrogen, U.S.A); yeast RNA (cat# 55714, Calbiochem, U.S.A); sodium dodecyl sulfate (cat# BP166-500, Fisher Scientific, China); RNase A (cat# 21210, Affymetrix, U.S.A); FM 5-95 (N-(3-Trimethylammoniumpropyl) -4-(6-(Diethylamino)phenyl) hexatrienyl) Pyridinium Dibromide), (Cat# T23360); fluorescent latex beads (cat.no. 1493, ApogeeMix, U.K), bare silica capillary with O.D. 362.0 μm and I.D. 75.3 μm (cat. no. TSP075375, Phoenix, AZ, USA). All buffers and samples were prepared from nuclease-free deionized water using a Synergy UV system (cat. no. SYNSV00WW) supplied with a 13 kDa cut-off, BioPak Point-of-Use ultrafilter (cat. no. MPGP02001, Millipore, MA, USA).

3.2.2 EVs staining and lysis

EVs were stained with YOYO-1 dye to perform further quantification experiments. For staining, EVs were incubated with 2 μM of YOYO-1 for 30 min at RT according to the manufacturer's protocol. Yeast RNA was stained with 2 μM of YOYO-1 for 30 min at RT and used as standard RNA for the calibration curve,

Chemical lysis of EVs was performed using 0.1% SDS. Ribonuclease A (RNAse A) 378 μg/mL was used to eliminate the free form of RNA from the EVs.

3.2.3. Calibration curve and standard addition plots

A calibration curve of yeast RNA was built in order to quantify the RNA content of EVs isolated from cancer cells. The standard RNA was diluted into a variety of concentrations between 1.5×10^{-2} to 1.0×10^{5} ng/mL. A solution of 2 μM of YOYO-1 was used for RNA staining. A calibration curve of standard RNA was built to determine the RNA concentration of EVs.

For EVs sample from urine, the standard addition method was used to avoid the matrix effect, hence, to precisely quantify RNA content of urine EVs. First, each EV sample was heated up at 95℃ for 2 h, in order to eliminate nuclease potentially present in the EVs sample after ultracentrifugation. Second, for each 50 μL of EVs sample after heating up, 6 aliquots of standard RNA were transferred in each EVs sample, followed by the addition of PBS solution in order to obtain a final volume of 60 μL. The RNA concentrations of each sample are 0, 0.0521, 0.137,0.231, 0.289, 0.370, and 0.479 ng/μL. The YOYO-1 (2 μM) was used for RNA staining. The standard addition plot was built using YOYO-1 stained urine EVs samples, and standard RNA was built to determine the RNA concentration of EVs. Chemical lysis of EVs was performed using 0.1% SDS.

3.2.4. Capillary Electrophoresis

A ProteomeLab PA 800 system (Beckman Coulter, CA, USA) was used to perform all capillary electrophoresis with laser-induced fluorescence detection (LIF). Fluorophores were excited using 488 nm Argon Ion Laser source (Beckman Coulter, CA, USA), in which fluorescence was detected using a 520±10 nm filter. The data were acquired and analyzed using 32 Karat Software version 8.0 (Beckman Coulter, CA, USA). The electrophoresis was performed using a fused silica capillary with a total length

of 59.1 cm and an effective length of 49.0 cm from the point of injection to the detection window. For electrokinetic separation experiments, a plug of 50 nL sample was injected into the capillary by applying a pressure pulse of 1.0 psi for 5 seconds. The analytes in the sample were separated by applying 25.1 kV potential difference along the capillary resulting in an electric field of 424 V/cm. To determine the total fluorescence of samples, a continuous plug was pushed through the capillary by applying 1.5 psi pressure for 10 minutes. The capillary was maintained at a temperature of 15°C at all times. The run buffer for all analyses was 25 mM borax buffer; before each run, the capillary was rinsed by applying 20.0 psi of 0.1 M HCl, 0.1 M NaOH, and dH2O for 2 minutes each and 25 mM borax buffer for 4 minutes. All buffers and rinsing solutions were passed through a 0.2 µm filter before use.

3.2.5. Flow cytometry

Beckman Coulter MoFlo Astrios EQ was adapted and optimized to nanoscale particle detection. The buffers were filtered by 3kDa (Amicon® Ultra-15 Centrifugal Filter Units) before using to reduce backgrounds. For the validation of selected EVs, isolated exosomes were subsequently incubated in the dark for 20 min with two dyes: YOYO-1 and FM 5-95. Control samples included unstained EVs samples and pure buffer samples. The data from flow cytometry were analyzed using the Kaluza analysis software.

3.3 Result and discussion

3.3.1 Separation of EVs by CE

In principle, EVqCE relies on the differential mobility of negatively charged free nucleic acids and intact EV particles. The general scheme of the method is depicted in Figure 3.1 and can be summarized as follows. After the ultracentrifugation, an EV-enriched sample is collected and stained with YOYO-1 fluorescent dye and subjected to capillary zone electrophoresis. YOYO-1 is a fluorogenic molecular probe binding to DNA and RNA. Once bound, it emits a bright green fluorescence at low concentrations. It also shows a high affinity to nucleic acids with little or no interaction with proteins and organelles. However, without biding to nucleic acids, there is little or no fluorescence. Here, I used YOYO-1 to stains both RNA and DNA, not only the one encapsulated in the vesicle core but also to the free nucleic acid released during the EV isolation process. The EV vesicles, as well as free nucleic acids, were subjected for the following EVqCE experiments and separated into two distinct zones. EVs vesicles travelled faster to the cathode than nucleic acids due to its smaller charge and bigger size and migrated slightly slower than an electroosmotic flow of the buffer solution, while free nucleic acids moved slower than EV vesicles. (**Figure 3.1 A**). After lysis by SDS, the peak representing EVs fraction disappeared, and the free nucleic acid peak increased. This increment corresponding to the total amount of encapsulated nucleic acid in intact EV was released into solution. (**Figure 3.1 B**)

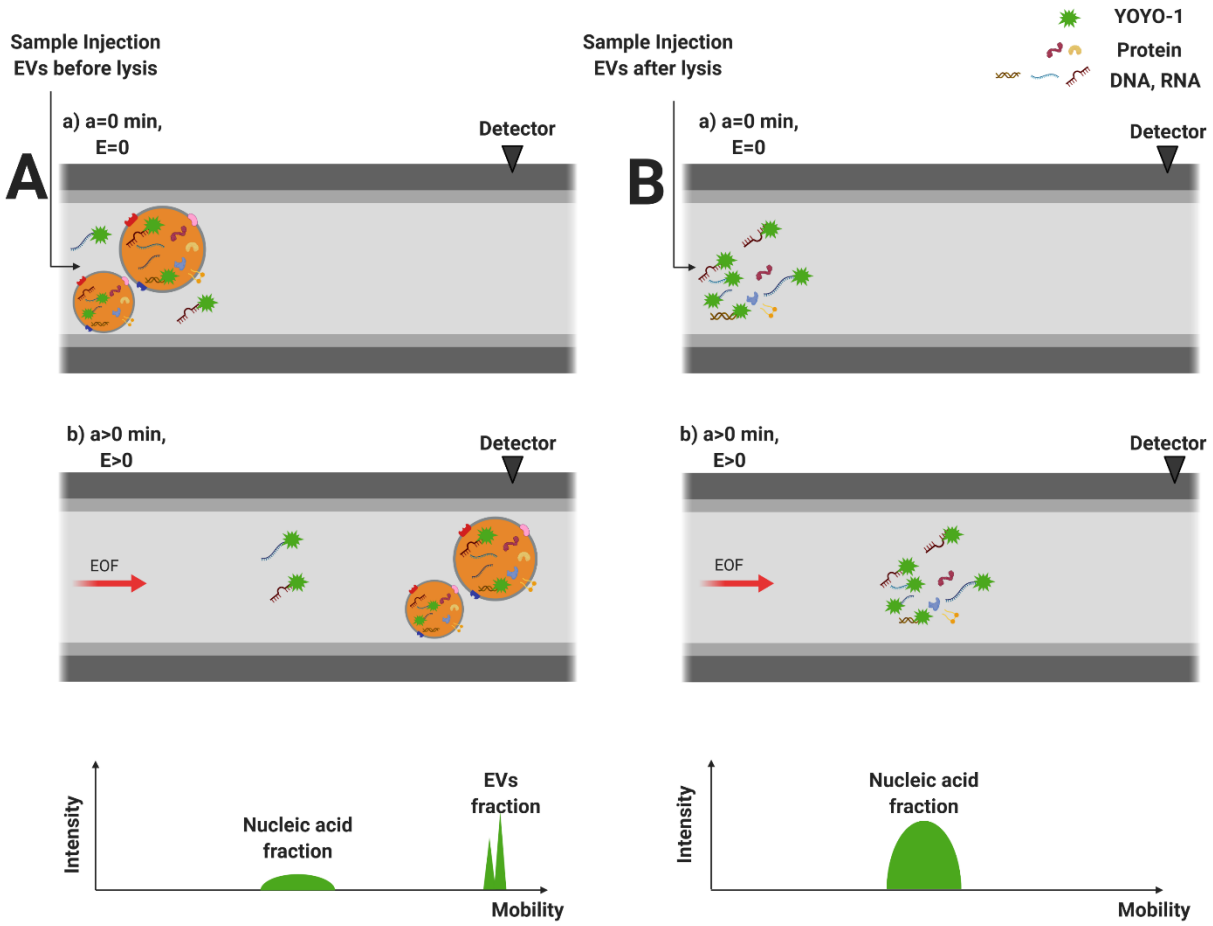

Figure 3.1. Schematic representation of qCE analysis for EVs from human urine. (A) A mixture of intact EVs with encapsulated nucleic acid and the free nucleic acid is stained with YOYO-1 (green stars) and injected into the capillary as a short plug. The electric field was applied (E > 0 V/cm), EVs and the free nucleic acid are separated into two fractions depending upon their mobility. (B) After lysis by SDS, the peak representing EVs fraction disappeared, and the free nucleic acid peak increased.

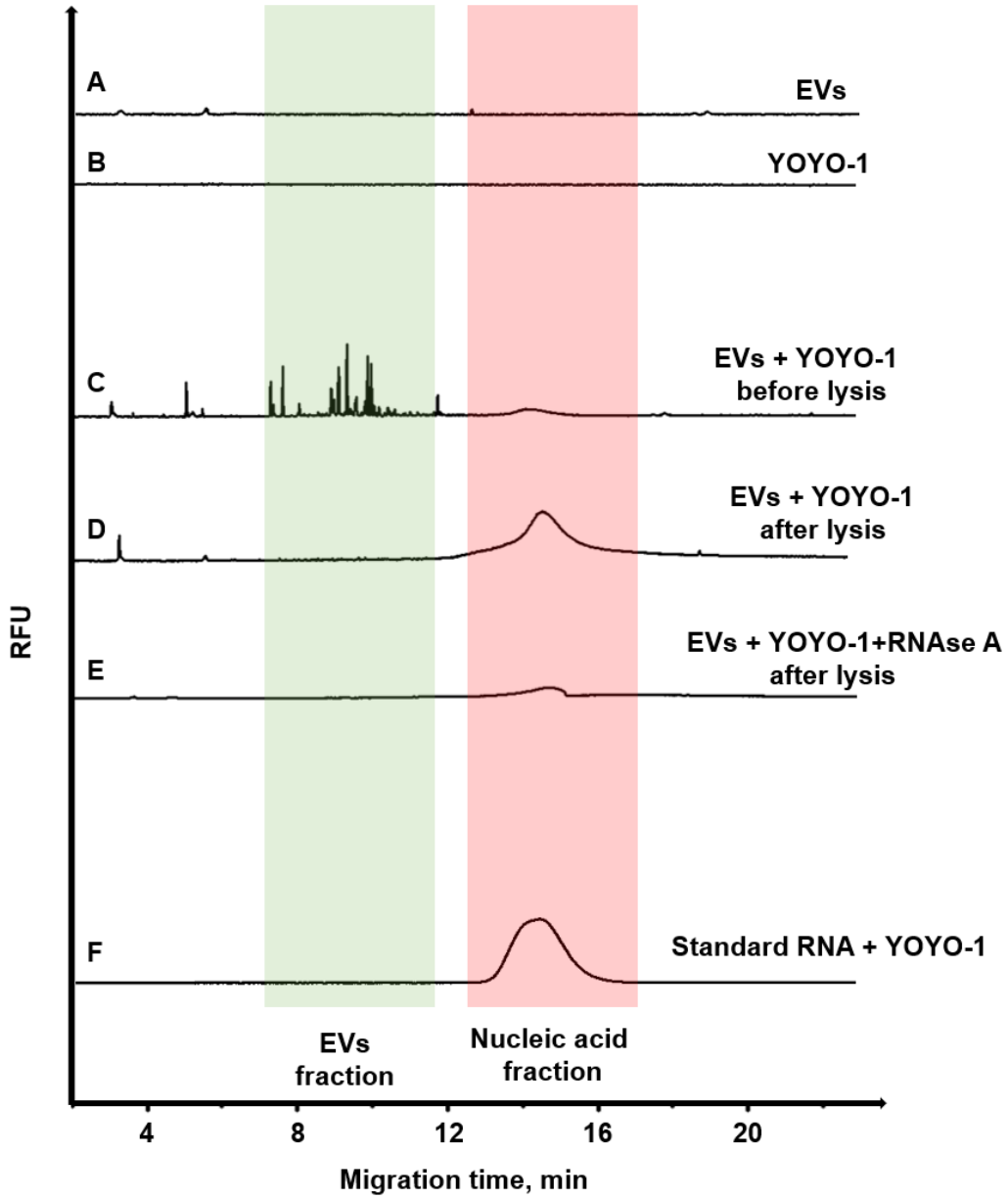

Figure 3.2 Experimental EVqCE electropherograms of EVs from cancer cells. (A) 2μM YOYO-1 only and (B) EVs without YOYO-1. (C) A sample of enriched EVs from MDA-MB-231 cells with encapsulated RNA. (D) After lysis by 0.1% SDS, the EV fraction decreases, and the nucleic acid peak increases. (E) After RNase treatment, RNA is hydrolyzed, leaving DNA only. DNA and RNA are stained with YOYO-1 dye and detected by LIF. (F) 150 ng/mL yeast RNA with YOYO-1.

3.3.2 RNA quantification of EVs from cancer cells

The control experiments were performed with individual CE analysis of YOYO-1 and EV (**Figure 3.2 A and B**). No significant peaks were observed because YOYO-1 and EVs did not fluoresce at 520 nm alone when they were excited at 488 nm. Then EVs were mixed with YOYO-1 and subjected for CZE separation. After the separation, two main florescent zones were observed corresponding to EVs stained with YOYO-1 and free nucleic acids stained with the dye, respectively (**Figure 3.2 C and F**). The free nucleic acid showed a wide peak, while the EVs demonstrates sharp peaks due to the larger particle size of EVs with low diffusion coefficients. It was difficult to quantify EVs directly because they produced multiple sharp peaks or spikes on an electropherogram resulting in irreproducible patterns. Moreover,

RNA-protein aggregates may contribute to those spikes, make them difficult to quantify EVs. Thereafter, I lysed EVs particles by SDS and observed the increase of the nucleic acid peak. The lysis of EVs was confirmed by the disappearance of the majority of spiked peaks corresponding to the intact EVs (**Figure 3.2 D**). The main contributor to the gain of the nucleic acid peak was RNA because, after the following RNAse treatment, the gain of the signal from nucleic acids disappeared completely (**Figure 3.2 E**). The electropherograms for EVs isolated from NCI-H1975 and CCL-119 cell lines were very similar to **Figure 3.2.** The results are shown in supporting information. (**Figure S2**)

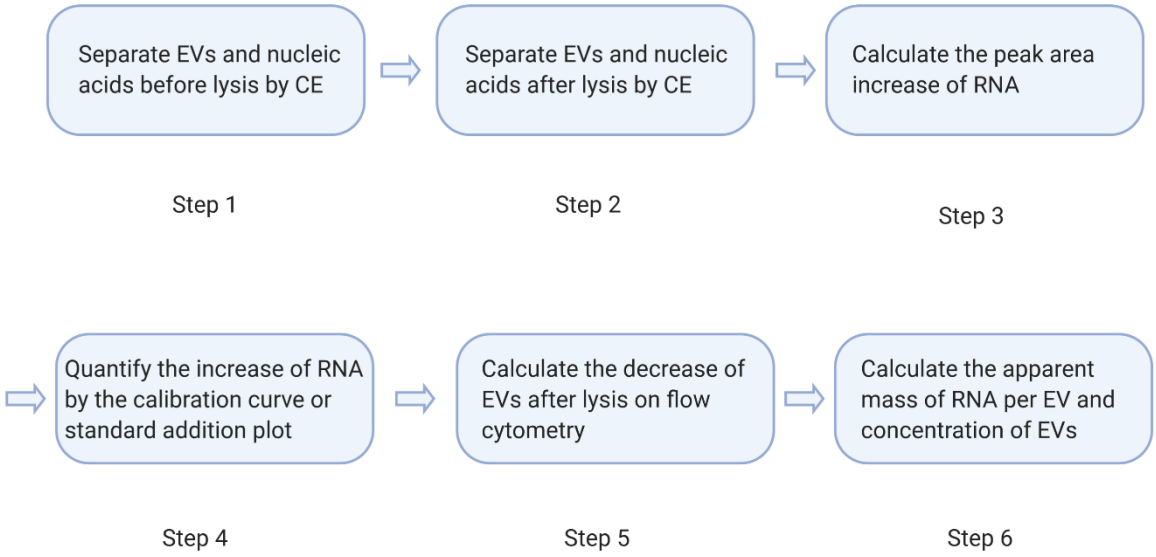

Figure 3.3 Schematic representations of calculation of EVs concentration.

The concentration of EVs was calculated in six steps, as shown in **Figure 3.3**. First, the EVs sample was stained with YOYO-1 was separated in CE. The observed nucleic acid fraction contains free RNA and DNA from degraded EVs and cells (**Figure 3.1 A**). Second, the EV sample was lysed with SDS, stained with YOYO-1 and separated again (**Figure 3.1 B**). Third, after lysis, the resulted nucleic acid fraction contains mainly RNA and a small amount of DNA from impurities and lysed EVs. ΔA_{RNA} is defined as the peak area of released RNA from EVs. It is calculated by determining the area of the nucleic acid peak before (A) and after SDS treatment with RNase A as in equation 3.1

$$\Delta A_{RNA} = (A_c - A_D) - (A_A - A_B) \quad (3.1)$$

A_A, A_B, A_c and A_D are the peak areas of the nucleic acid of (A), (B), (C) and (D), respectively. (**Figure 3.4**)

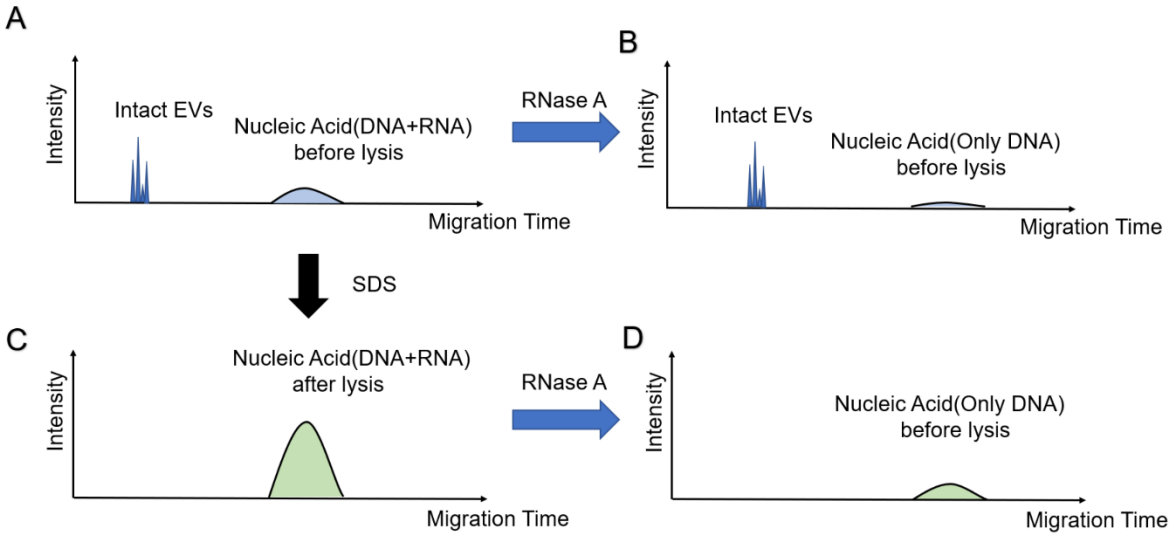

Figure 3.4 Schematic illustrates the RNA quantifications by EVqCE. EVs were stained with YOYO-1 (A) EVs without any treatment. (B) RNAse A treated EVs depicting the degradation of RNA. (C) SDS treated EVs showing the degradation of intact EVs and the increase in the intensity of the peak for nucleic acid. (D) SDS and RNase A treated EVs showing the degradation of RNA.

The fourth step is the quantification of ΔA_{RNA}. A calibration curve was built by plotting fluorescent intensities of RNA standards stained by YOYO-1 as a function of their concentrations (**Figure 3.5**). The fluorescent intensities of the standards were measured by the same LIF detector and CE instrument. The concentration of the released RNA in one unknown EV sample after lysis could be acquired by measuring the peak area in the form of a relative fluorescence unit (RFU) from an RNA fraction, which corresponding to a certain concentration in the curve. The relationship between RFU and concentration of standard RNA on the calibration curve in **Figure 3.5** can be modelled by the following formula in origin 9.0 software. Error bars for each sample are acquired by three technical replicates on CE in the same condition (**Figure S3 A**).

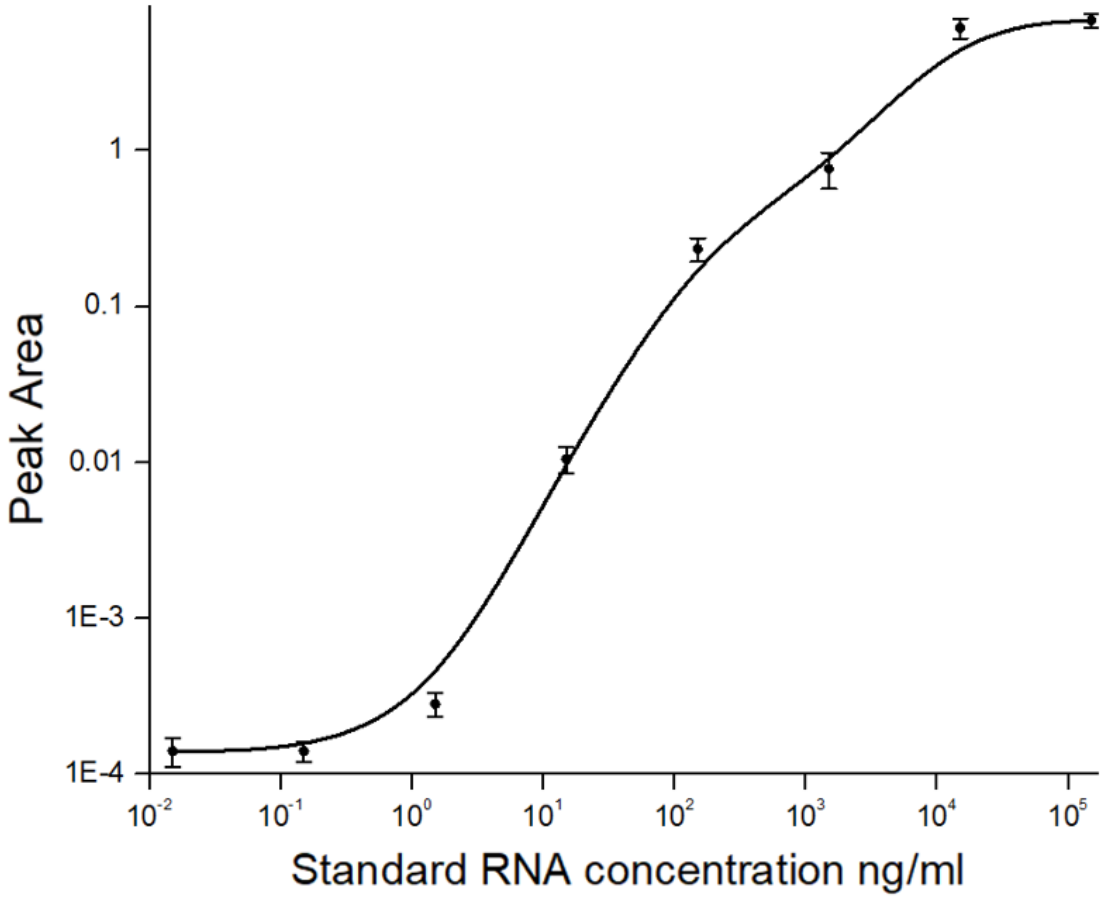

Figure 3.5 Calibration curve of YOYO-1-stained standard RNA to determine the RNA concentration of EVs. A solution of 2μM of YOYO-1 was used for RNA staining. RFU values were calculated by integration in the Origin 9.0 software.

When $10^1 \leq x \leq 10^3$ ng/mL, as in equation 3.2:

$$y = -132.11 + 433.11e^{(x-1)/259.8} \tag{3.2}$$

When $10^3 < x \leq 10^5$ ng/mL, as in equation 3.3:

$$y = 1.62 - 1.43e^{\frac{x-5888.95}{45418.5}} \tag{3.3}$$

The concentration of unknown RNA can be found from the calibration curve. Steps five and six of EV calculation will be further explained in **section 3.3.4.**

3.3.3 RNA quantification of urine EVs

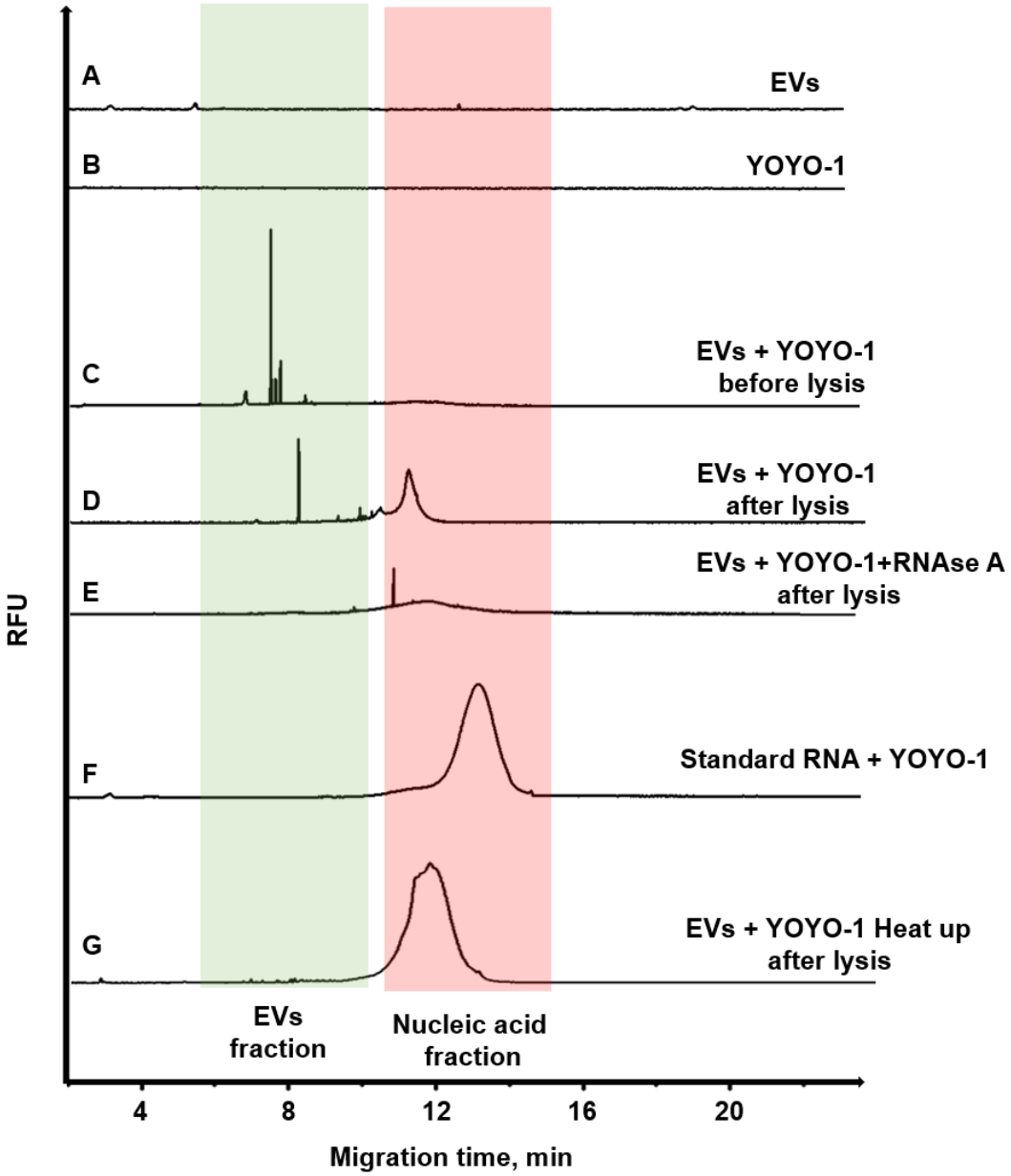

Figure 3.6 Experimental EVqCE electropherograms of EV from urine. (A) 2 μM YOYO-1 only and (B) EVs without YOYO-1. (C) A sample of enriched EVs from urine. (D) After lysis by 0.1% SDS (E) After RNase treatment, RNA is hydrolyzed, leaving DNA only. DNA and RNA are stained with YOYO-1 dye and detected by LIF. (B5) Standard RNA with YOYO-1. (G) After heating up at 95℃ for 2 hours and lysis by SDS, the EV fraction disappears, and the nucleic acid peak increases. The gain shows the amount of released RNA and is used to count EVs.

Compared with the result of EVs from cancer cells, the electropherogram pattern of EV from urine is quite similar to cancer cells (**Figure 3.6**). However, two points need to be discussed. First, it is difficult for spikes from EVs fraction to be eliminated completely, especially for EVs from urine. This is probably because some aggregates that contain nucleic acids can be stained by YOYO-1 but show resistance to SDS. Second, I observed that the nucleic acid peak was quite insignificant compare to the one from cancer cell EVs (**Figure 3.6 D**). Technically, the free nucleic acid started to degrade over time once the lipid membrane was solubilized by SDS. This is because EV samples were collected from the

urine; the nuclease still existed after centrifugation.

In this case, the peak area of nucleic acid in the electropherogram is improper for the calculation. To confirm the presence of nuclease in urine EV samples and precisely analyze RNA content from urine EVs, each EV sample was respectively heated up at 95℃ for 0, 30, 120 min before lysis, and calculated their peak area of RNA. Six samples were incubated in RT for 30, 60, 90, 120, 150, 180 min to monitor the effect of potential nuclease on released RNA. The initial detection time was set at 30 minutes. It took around 30 mins, including treating an EV sample and migration time in the capillary. (**Figure 3.6**) The sample without heating showed the lowest initial RFU and significantly decreased over incubation time, which showed the existence of nuclease. (**Figure 3.6 A**). The 30 min heating showed a higher initial RFU and, 2 hours heating showed a completed elimination of nuclease activity (**Figure 3.6 B, C**). The removal of nuclease led to a larger peak of nucleic acid (**Figure 3.6 G**). Therefore, heating EV samples for 2 hours before lysis helped in the quantification of EVs from urine.

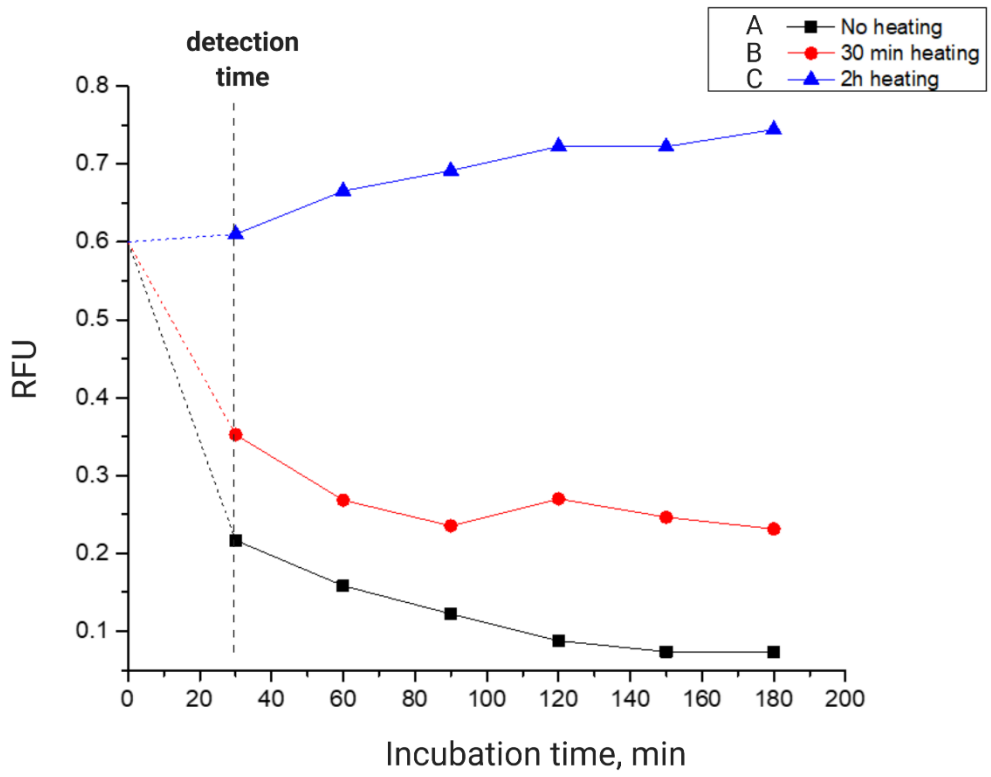

Figure 3.7 Effect of heating on the stability of released RNA from urine EVs.

In view of the complexity of EV samples collected from urine, the standard addition method rather than calibration curve was used to avoid a matrix effect, hence provides a much convincing value during the calculation of ΔA_{RNA}.(**Figure 3.8**) Error bars for each sample are acquired by three technical replicates on CE in the same condition.

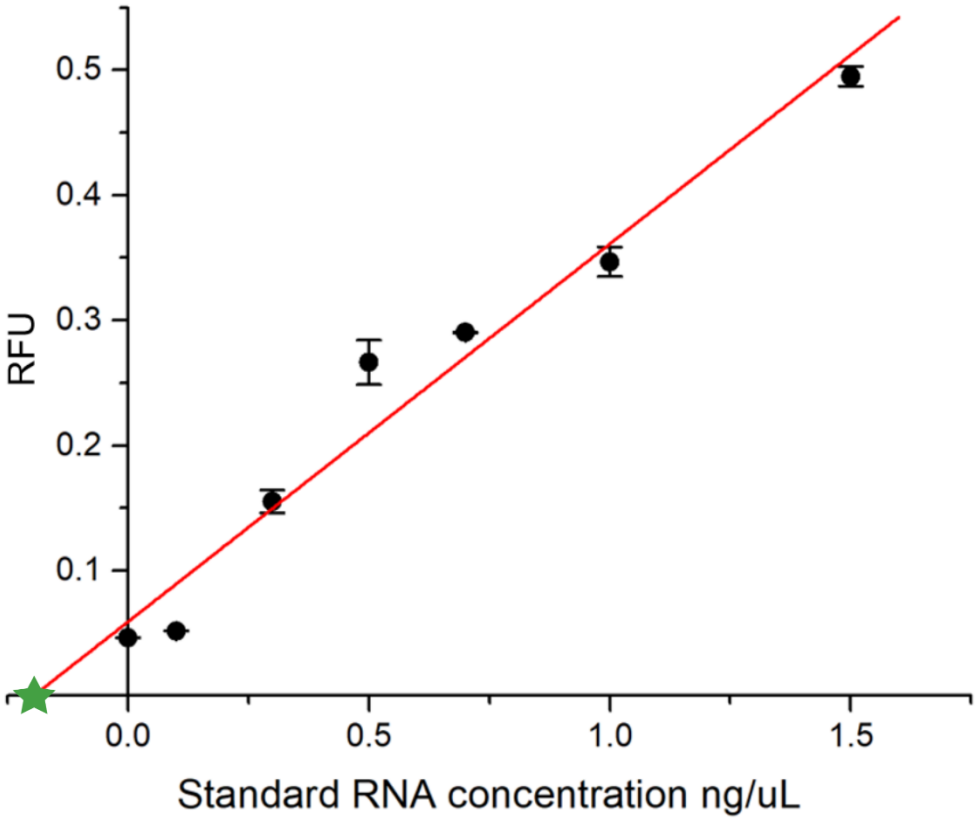

Figure 3.8 The standard addition plot of YOYO-1-stained EVs with standard RNA to determine the RNA concentration of EVs. A solution of 2 μM of YOYO-1 was used for RNA staining. The Peak Area Unit value was calculated by the integration in Origin 9.0 software. The value of the green asterisk on the x-axis indicates the concentration of RNA in EVs sample (-0.196, 0).

The fluorescent intensities were measured by continuous flow as in equation 3.4:

$$y = 0.302x + 0.0592 \quad (3.4)$$

In this formula, x is the concentration of standard RNA added into the EVs sample, while y is the peak area unit of RNA peak on CE. The absolute value of the x-intercept (green asterisk in **Figure 3.8**) is the concentration of encapsulating RNA in the EVs sample, which equals to 0.196 ng/μL.

3.3.4 EV quantification by flow cytometry

In the fifth step, the concentration of intact EVs was found by flow cytometry. FM dyes are lipophilic styryl compounds used in a variety of labelling purposes, including the plasma membrane and vesiculation.[121] To label intact EVs before testing, FM 5-95 was used to mark the lipid membrane of EVs, while YOYO-1 stained capsulated nucleic acids. The treatment of SDS caused the partial elimination of YOYO-1 and FM 5-95 positive events.

Particles stained by FM 5-95 and YOYO-1 were counted as intact EVs (**Figure 3.9**). After the treatment of 0.1% SDS, the FM 5-95 and YOYO-1 positive events decreased significantly because of EV lysis.

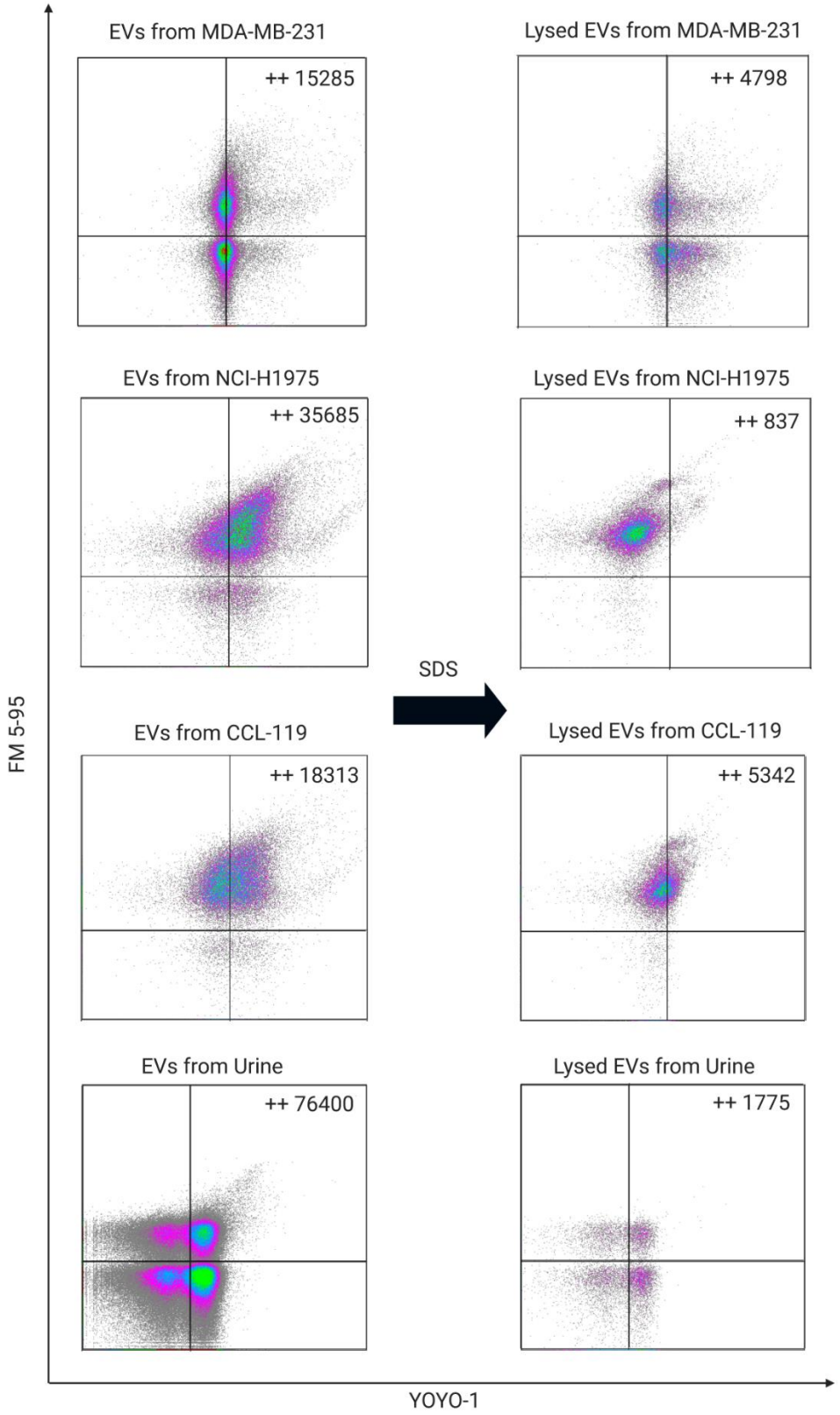

Figure 3.9 Flow cytometry analysis of EVs before and after the SDS treatment. EVs were stained and gated by anti-CD63 APC and anti-CD9 PE antibodies. The lysis process was performed by 0.1% SDS. The number of double positive (YOYO-1 and FM 5-95) events is shown at the top-right corner.

The number of events can be transformed into EV concentration if the average flow rate, $\bar{v}$. is known in flow cytometry. To find the flow rate, control nanobeads of 110nm were co-injected with EVs. The average flow rate (μL/s) was determined for a total of 71555 particles under 0.3 psi within 120 seconds and was found to be equal to 4.125×10^{-3} μL/s. That was the flow rate of EVs in the sample.

The concentration of EVs in a sample, $\Delta[EV], 1/\mu L$ was calculated from equation 3.5:

$$\Delta[EV] = [EV]_1 - [EV]_0 \tag{3.5}$$

$$[EV] = \frac{N_c}{\bar{v}t} \tag{3.6}$$

$[EV]_1$ and $[EV]_0$ are the concentration of EVs before and after lysis. N_c is the number of EV particles pass through the detector in time t.

3.4.5 EV quantification by CE

In the sixth step, the apparent mass of RNA per EV (M_{RNA}, g/particle) can be calculated from equation 3.7:

$$M_{RNA} = \frac{\Delta[RNA](10^{-9})}{\Delta[EV]} \tag{3.7}$$

$\Delta[EV]$ is the concentration ($1/\mu$L) of intact EVs in the sample determined by flow cytometry. $\Delta[RNA]$ is the increase of concentration of RNA (ng/μL) in the same EV sample after lysis determined by the calibration curve or standard addition plot in **Figure 3.6** and **Figure 3.7.** The final value of M_{RNA} for EVs from MDA-MB-231, NCl-H1975, CCL-119 and urine are $(1.96 \pm 0.3)\times10^{-13}$, $(3.75 \pm 0.4)\times10^{-13}$, $(3.33 \pm 0.2)\times10^{-13}$ and $(5.42 \pm 0.8)\times10^{-13}$ g/particle, respectively. For example, a typical mammalian cell contains around 2×10^{-11} g of total RNA. [122]

The concentration of intact EVs in an unknown EV sample [EVs]* can be calculated from equation 3.8:

$$[EV]^* = \frac{\frac{\Delta A^*_{RNA}}{\Delta A_{RNA}}\cdot[RNA](10^{-9})}{M_{RNA}} \tag{3.8}$$

To confirm the feasibility of EVqCE, EVs samples were studied by different quantification methods. The results from EVqCE analysis, Nanoparticle tracking (NTA) and flow cytometry are summarized in **Table 3.1**. Errors for each sample are acquired by three biological replicates on CE in the same condition **(Figure S3 B, Table S1)**. The concentrations from EVqCE were calculated using formula 3.8, while the concentrations of EVs from flow cytometry were based calculated using formula 3.6. The EV concentrations from NTA was acquired directly from NTA reports. The majority of NTA results showed higher concentrations of EVs due to additional counting of non-EV particles. Flow cytometry showed lower concentrations due to missing of the EV population smaller than 100 nm. The flow cytometry scattering detector could not recognize very small particles.

Table 3.1 Quantification of EVs performed by EVqCE, NTA and flow cytometry (antibodies).

Quantification Method	MBA-MB-231	NCl-H1975	CCL-119	Urine
EVqCE (particles/mL)	$(5.1 \pm 0.2) \times 10^9$	$(1.4 \pm 0.1) \times 10^9$	$(1.3 \pm 0.4) \times 10^9$	$(3.6 \pm 0.6) \times 10^9$
NTA (particles/mL)	$(4.9 \pm 0.1) \times 10^{10}$	$(2.3 \pm 0.2) \times 10^{10}$	$(2.6 \pm 0.3) \times 10^{10}$	$(1.3 \pm 0.3) \times 10^{11}$
Flow cytometry (particles/mL)	$(1.7 \pm 0.3) \times 10^9$	$(3.6 \pm 0.7) \times 10^8$	$(6.0 \pm 0.8) \times 10^8$	$(2.5 \pm 0.4) \times 10^9$

3.5 Conclusion

In this chapter, a method to quantify EVs was developed. I found that RNA was the most abounded nucleic acid in EVs. First, EVs from MDA-MB-231, NCl-H1975, CCL-119 and urine were stained with the RNA/DNA dye, YOYO-1. After the separation of EVs in CE, two zones of peaks of EVs and RNA were observed. Yeast RNA was selected as a standard to quantify EVs, so the area of RNA peak from CE was transformed into RNA concentration. Next, EVs were stained with YOYO-1 and FM 5-95 and tested in flow cytometry to determine their concentration of EVs. By comparing the ratio of the decrement of intact EVs corresponding to increment of free RNA, an apparent mass of RNA in EV particles was calculated. After, I estimated the amount of EVs simply by using the RNA concentration identified by CE. The results were compared with NTA and flow cytometry.

Chapter 4. Quality control of Extracellular Vesicles

4.1 Objective

The EV and other EV-liked particles, e.g., liposome, will decay not only under the treatment of detergent but also happens under different conditions. Herein, we extend the EVqCE into quality control of EVs to monitor their degradation process and its life span.

4.2 General procedure

Degradative conditions: EVs were exposed to the following conditions to determine the amount of degradation. Extensive vortexing: 50 µL of EVs were continuously vortexed for 5 minutes at the highest speed using an analog vortex mixer (VWR, Canada). Sonication: 50 µL of EVs samples were placed in a Branson Ultrasonic Cleaner (Model 3510, Branson Ultrasonics Corporation, USA) for 10 minutes at room temperature. Freeze-thaw cycles: 50 µL of EVs samples were exposed to 10 freeze-thaw cycles. This was performed by freezing the samples in -80^{0}C for 30 seconds and then allowing them to completely thaw at RT for 2.5 minutes.

4.3 Result and discussion

4.3.1 Degradation analysis of EVs from cancer cells

In equation 4.1, EVs degradation percentage (EVD) can be used to measure the level of EVs degradation by calculating the percentage of EV lysis, which means their RNA lost protection by intact EVs during processes commonly encountered during EVs storage or use.

$$EVD = \frac{C_A - C_B}{C - C_B} \cdot 100\% \quad (4.1)$$

C_A is the concentration of the RNA from EVs sample after the degradation process, while C_B is the concentration of RNA from EVs samples before the degradation process.C is the concentration of the RNA from EVs' original sample after 0.1% SDS treatment. This study aims to focus on the released RNA as a standard for degraded EVs. All the above values are quantified from equations 3.1, 3.2 and 3.3. The result of EVD was studied from a batch of EVs isolated from cancer cells after different treatments. **Figure 4.1** illustrates the electropherograms of EVs degradation after various treatments and storage conditions. Errors for each sample are acquired by three technical replicates on CE in the same condition.

Storage: To test the stability of EVs in storage, two samples were stored at 4 ℃ for 7 and 14 days. A degradation level of 32.4% ± 6.5 of EVs was observed at 14 days storage, which is higher than the one at 7 days (3.1% ± 0.9). (**Figure 4.1 A, B**)

Extensive vortexing: Vortexing is another commonly used procedure for solubilizing insoluble components or pellets after centrifugation. The same analysis, as described above, was applied to samples vortexed continuously for 5 minutes. The mild treatment for 30 seconds only slightly, 4.7±1.8%, degraded the EVs. (**Figure 4.1 C**)

Freeze-thaw cycles: Storage of biological samples at very low temperatures pose a risk associated with loss of activity or degradation attributed to cycles of freezing and thawing. After 10 cycles, 40.3 ± 7.0% of EVs degradation was observed. (**Figure 4.1 D**)

Ultrasonic treatment: A long time sonication or ultrasonic treatment is often used as a technique for producing lipid vesicles, while short and strong sonication or ultrasonic treatment would cause a breakdown of EVs. Therefore, we analyzed the effects of ultrasonic treatment on EVs using an ultrasonic bath with 40 kHz power. The EV sample was degraded by 85.7 ± 25.8% after 10 minutes of

treatment. It is worth mentioning that EVs treated with sonication showed a higher fluorescent signal than the one with 0.1% SDS sometimes. This is probably because sonication allowed the permeability in the lipid bilayer membrane of EVs; hence the YOYO-1 dye is able to enter inside and bind to the nucleic acids. (**Figure 4.1 E**)

The study demonstrated that the mechanical processes of vortexing and sonication seem to promote RNA release much more than freezing and thawing of the sample.

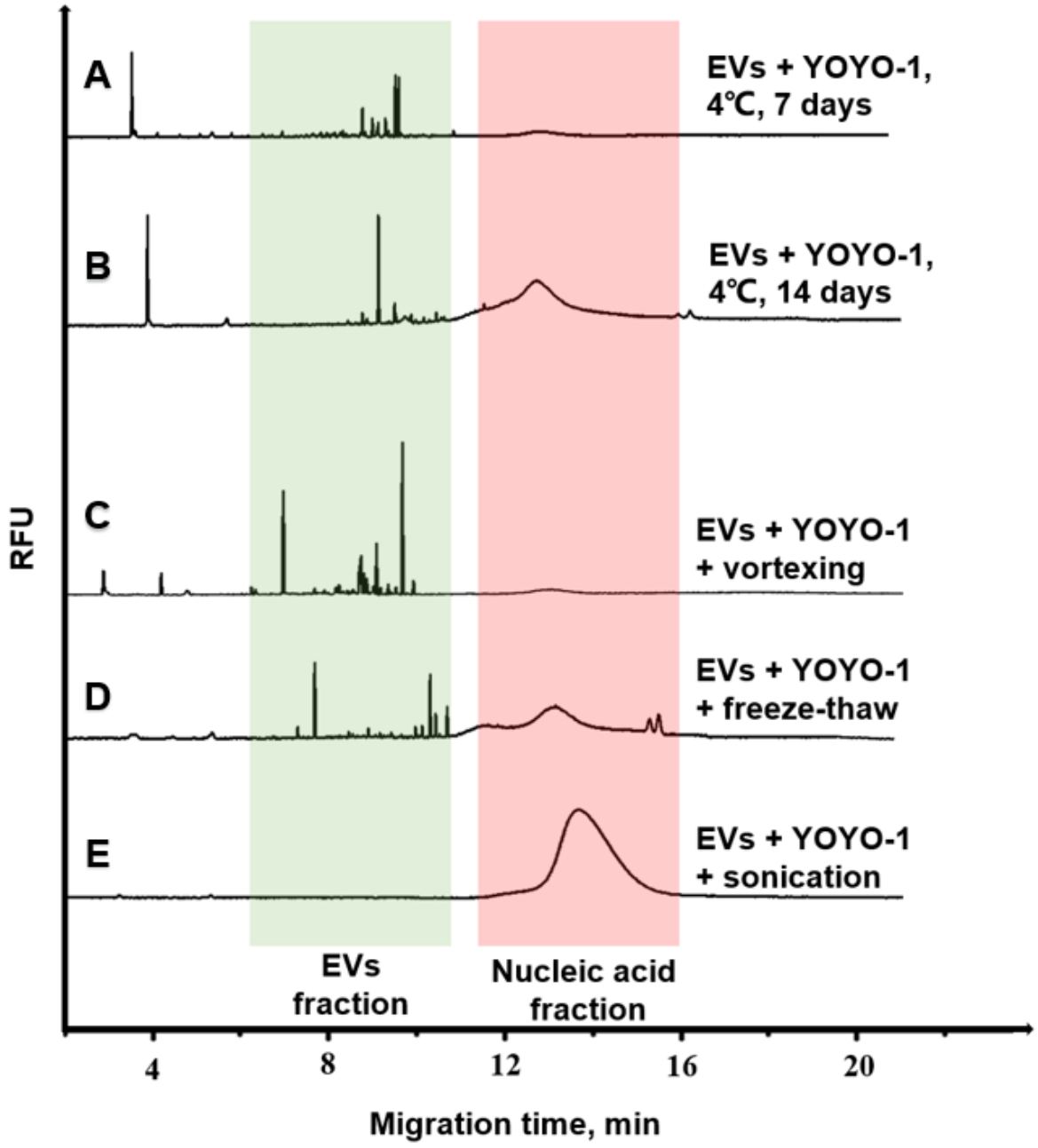

Figure 4.1 Experimental EVqCE electropherograms of degradation analysis of EVs isolated from cancer cell lines. Effect of storage temperature on EVs stored at 4˚Cfor 7 days (a); Effect of storage temperature on EVs stored at 4˚C for 14 days (b); Effect of storage temperature on EVs stored at 4˚C for 7 days (c); EVs stained with YOYO-1 treated with 10 min vortexing (d); EVs with YOYO-1 treated with 10 freeze-thaw cycles (e); EVs with YOYO-1 treated with 10 min sonication.

4.3.2 Degradation analysis of EVs isolated from urine samples

EVs degradation percentage (EVD) can also be used to measure the level of EVs degradation by calculating the percentage of EV lysis, which means their RNA lost protection by intact EVs during processes commonly encountered during EVs storage or use. The calculation is different from the EVs from cancer cells, as in equation 4.3.

$$EVD = \frac{C_B{}' - C_A{}'}{C' - C_B} \cdot 100\% \quad (4.3)$$

$C_A{}'$ is the concentration of the RNA from unknown EVs sample after the degradation process and then treat with 2 hours heating at 95 ℃, followed by 0.1% SDS.$C_B{}'$is the concentration of RNA from EV samples before the degradation process, followed by 0.1% SDS with 2 hours heating at 95 ℃. C' is the concentration of the RNA from EVs original sample after 0.1% SDS treatment with 2 hours heating at 95 ℃? Due to the presence of nucleases in the EVs collected from the urine sample, the quantification of EVD is followed, which is different from the one in cancer cells. This aims to focus on the RNA protected by the lipid membrane as a standard of surviving EVs. All the above values are to be calculated from the equation 3.1 and 3.4. The result of EVD was studied from a batch of EVs isolated from urine after different treatments. **Figure 4.2** illustrates the electropherograms of EV degradation after different treatments and storage conditions. Errors for each sample are acquired by three technical replicates on CE in the same condition.

Storage: Three EV samples isolated from urine were stored at 4 ℃ for 7,14 and 21 days. The degradation level of EVs is 3.5 ± 2%, 31 ± 3.5% and 59 ± 4.3%. (**Figure 4.2 A, B, C**)

Extensive vortexing: The same analysis, as described above, was applied to the EV sample isolated from urine vortexed continuously for 5 minutes. The mild treatment of 30 seconds only slightly, 10.4 ± 1.2%, degraded the EVs. (**Figure 4.2 D**)

Freeze-thaw cycles: The same analysis, as described above, was applied to the EV sample isolated from urine after 10 freeze-thaw cycles, 65.9 ± 3.6 % of EVs degradation was observed. (**Figure 4.2 E**)

Ultrasonic treatment: The same analysis, as described above, was applied to the EV sample isolated from urine after 10 minutes of treatment, showed a degradation level of 73.8 ± 10.4 %. (**Figure 4.2 F**)

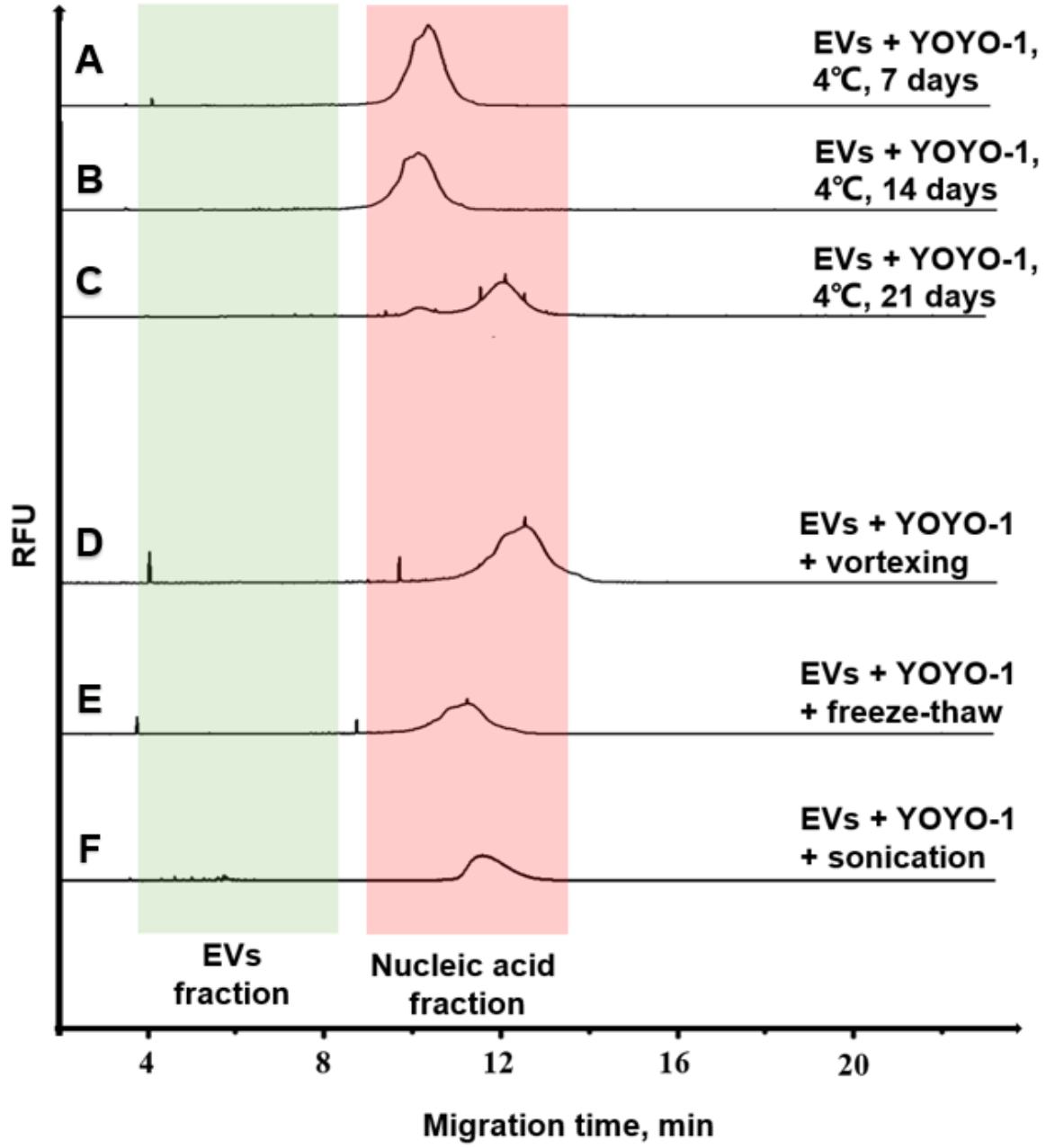

Figure 4.2 Experimental EVqCE electropherograms of degradation analysis of EVs isolated from urine. EVs stored at 4˚Cfor 7 days (A); EVs stored at 4˚C for 14 days (B); EVs stored at 4˚C for 21 days (C); EVs stained with YOYO-1 treated with 10 min vortexing (D); EVs withYOYO-1 treated with 10 freeze-thaw cycles (E); EVs with YOYO-1 treated with 10 min sonication (F).

4.4 Conclusion

EVqCE also provides a facile way to investigate the level of EVs degradation without the need for quantification of the total amount of EV present in each sample due to the separation of intact EVs particles from free nucleic acids. Thus, the gain in the area under the nucleic acid peak after a given degradative process can be used as a measure of the degradation level. This is a promising study which is able to provide the guideline suggestion to EV-based drug carrier design.

Chapter 5. General discussion and conclusion

In this study, we have successfully isolated EVs from three cancer cell lines such as MDA-MB-231, NCl-H1975, CCL-119, as well as human urine by ultracentrifugation. The ultracentrifugation method was optimized, and the EVs are characterized using different techniques, including, i.e. TEM, NTA and flow cytometry. EVs showed the membrane-based structure, a size between 30-200 nm and labelled with anti-CD9 and anti-CD63 significantly indicated the good presence of surface biomarker on EVs. Then CE has been performed to separate the EVs and nucleic acid by labelling the EVs with YOYO-1. The method of determining EV concentration was built by six steps. The results were compared with NTA and flow cytometry, which are the most commonly used methods for EVs quantification. Last, the quality control study has been performed, demonstrated that CE could also be utilized on monitoring the quality of EVs under different critical conditions. The above-mentioned study suggests the workability and reproducibility of EVqCE. EVqCE allows a fast (~20 min) quantification of EVs in an unknown sample. To the best of our knowledge, for the first time, our study demonstrated a quantitative method of EVs using CE. Further, this study also provided information about the apparent mass of RNA in a single EV (M_{RNA}, g/particle) using the CE method. The EVqCE provided a rapid method to separate intact EVs particles and free nucleic acids and to calculate the level of EVs degradation and quantification. This method is relatively inexpensive and simple to operate, without any sample pre-treatment and can usually be completed in less than an hour. In addition, another advantage of EVqCE is that it requires less sample volume (25-50 μL), which provides benefits for the analysis of the fetal sample and other precious body fluid. The quality control process is also easy and rapid. This technology provides the possibility of real-time monitoring of EVs and the quantification content, which would lead to great application prospects in future EVs research and rapid quality testing in pharmaceuticals and biomedical applications. On the other hand, several limitations should be addressed before the method is fully utilized on an industrial scale. The CE method is unable to distinguish and separate EVs between each other. The quantification of EVs requires an additional test by flow cytometry. Apart from this, EVqCE depends on the RNA content from EVs, which means that extra care should be taken to ensure the stability of RNA. Finally, EVqCE needs at least 20 min for each run. To make this method more useful, it will require more optimization with different body fluid samples for future clinical use.

Overall, EVqCE demonstrated the lysis of EVs with minimum sample loss. EVqCE will be beneficial for future studies due to the biological significance of EVs. The future work may be centred on the application of EVqCE on original and untreated samples from cell-cultured media, stem cell-derived exosomes and different body fluid. Furthermore, the study on using EVqCE to distinguish different populations of EVs will be a significant application in biomedical fields.

Appendix

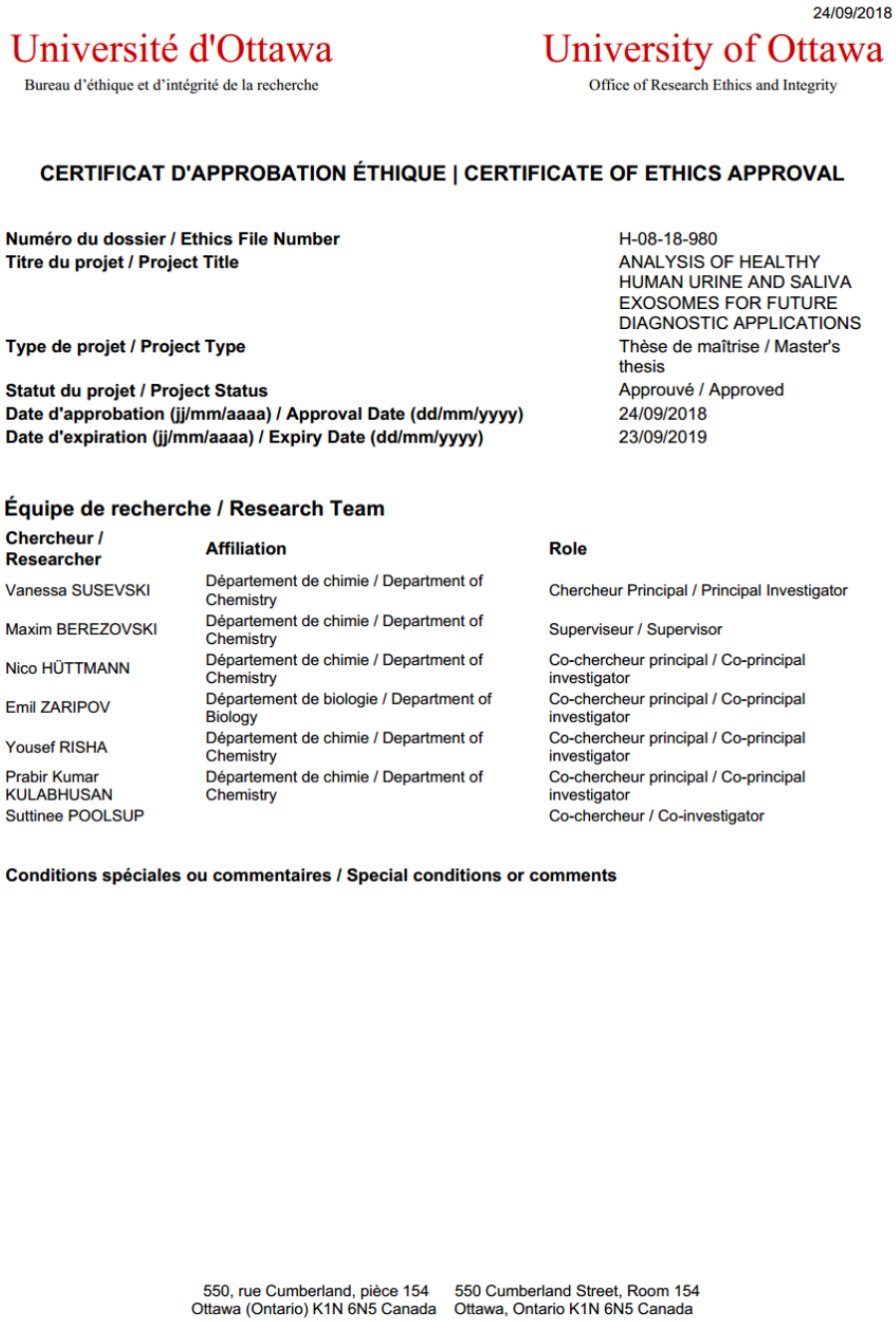

24/09/2018

Université d'Ottawa
Bureau d'éthique et d'intégrité de la recherche

University of Ottawa
Office of Research Ethics and Integrity

CERTIFICAT D'APPROBATION ÉTHIQUE | CERTIFICATE OF ETHICS APPROVAL

Numéro du dossier / Ethics File Number	H-08-18-980
Titre du projet / Project Title	ANALYSIS OF HEALTHY HUMAN URINE AND SALIVA EXOSOMES FOR FUTURE DIAGNOSTIC APPLICATIONS
Type de projet / Project Type	Thèse de maîtrise / Master's thesis
Statut du projet / Project Status	Approuvé / Approved
Date d'approbation (jj/mm/aaaa) / Approval Date (dd/mm/yyyy)	24/09/2018
Date d'expiration (jj/mm/aaaa) / Expiry Date (dd/mm/yyyy)	23/09/2019

Équipe de recherche / Research Team

Chercheur / Researcher	Affiliation	Role
Vanessa SUSEVSKI	Département de chimie / Department of Chemistry	Chercheur Principal / Principal Investigator
Maxim BEREZOVSKI	Département de chimie / Department of Chemistry	Superviseur / Supervisor
Nico HÜTTMANN	Département de chimie / Department of Chemistry	Co-chercheur principal / Co-principal investigator
Emil ZARIPOV	Département de biologie / Department of Biology	Co-chercheur principal / Co-principal investigator
Yousef RISHA	Département de chimie / Department of Chemistry	Co-chercheur principal / Co-principal investigator
Prabir Kumar KULABHUSAN	Département de chimie / Department of Chemistry	Co-chercheur principal / Co-principal investigator
Suttinee POOLSUP		Co-chercheur / Co-investigator

Conditions spéciales ou commentaires / Special conditions or comments

550, rue Cumberland, pièce 154
Ottawa (Ontario) K1N 6N5 Canada

550 Cumberland Street, Room 154
Ottawa, Ontario K1N 6N5 Canada

Figure S1. Certificate of ethics approval for analysis of healthy human urine and saliva EVs for future diagnostic applications.

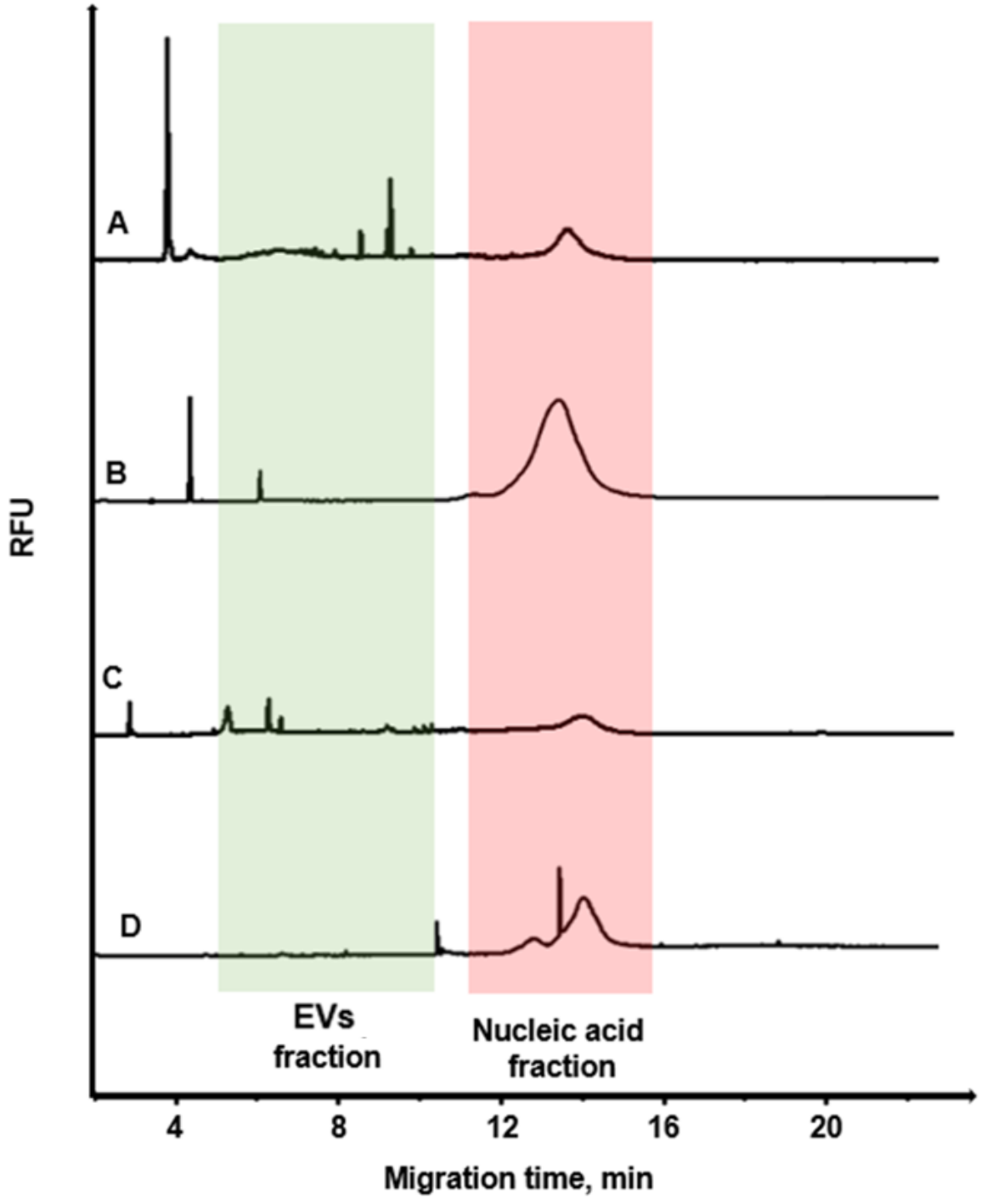

Figure S2. Experimental EVqCE electropherograms of EV from NCI-H1975 and CCL-119 cell lines. (A) A sample of enriched EVs from NCI-H1975 cell line. (B) Sample A After lysis by 0.1% SDS (C) A sample of enriched EVs from CCL-119 cell line. (D) Sample B After lysis by 0.1% SDS.

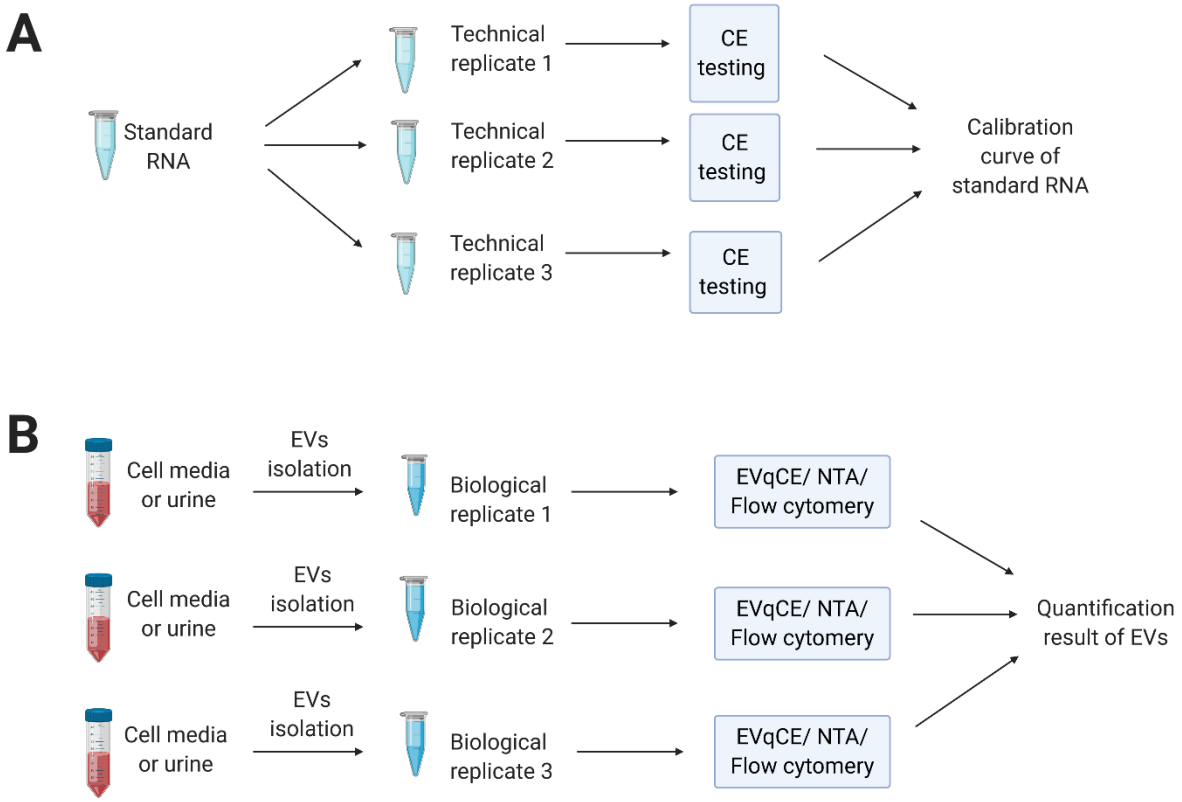

Figure S3. Experimental designs of technical replicates and biological replicates. (A) Technical replicates for building a calibration curve of standard RNA. (B) Biological replicates for quantification of EVs.

Table S1. Data on biological replicates in EVs quantification.

Quantification Method	MBA-MB-231	NCl-H1975	CCL-119	Urine
EVqCE (particles/mL)	4.9×10^9 5.2×10^9 5.1×10^9	1.4×10^9 1.4×10^9 1.5×10^9	1.0×10^9 1.2×10^9 1.7×10^9	3.3×10^9 3.2×10^9 4.1×10^9
NTA (particles/mL)	4.9×10^{10} 4.8×10^{10} 5.0×10^{10}	2.3×10^{10} 2.2×10^{10} 2.5×10^{10}	2.5×10^{10} 2.4×10^{10} 2.9×10^{10}	1.3×10^{11} 1.0×10^{10} 1.6×10^{10}
Flow cytometry (particles/mL)	1.5×10^9 1.6×10^9 2.0×10^9	3.4×10^8 3.1×10^8 4.3×10^8	5.2×10^8 5.5×10^8 6.4×10^8	2.4×10^9 2.9×10^9 2.2×10^9

Reference

1. György, Bence, Szabó, Tamás G *et al.* Membrane vesicles, current state-of-the-art: emerging role of extracellular vesicles. *Cell. Mol. Life Sci.* **68**, 2667-2688 (2011).
2. Choi, Dong-Sic.Urinary extracellular vesicles for biomarker source to monitor polycystic kidney disease. *PROTEOMICS–Clinical Applications* **9**, 447-448 (2015).
3. Akers, Johnny C, Ramakrishnan, Valya *et al.* Comparative analysis of technologies for quantifying extracellular vesicles (EVs) in clinical cerebrospinal fluids (CSF). *PloS one* **11**, e0149866 (2016).
4. Oosthuyzen, Wilna, Sime, Nicole EL *et al.* Quantification of human urinary exosomes by nanoparticle tracking analysis. *The Journal of physiology* **591**, 5833-5842 (2013).
5. Rupert, Déborah LM, Claudio, Virginia *et al.* Methods for the physical characterization and quantification of extracellular vesicles in biological samples. *Biochimica et Biophysica Acta (BBA)-General Subjects.* **1861**, 3164-3179 (2017).
6. Anderson, H Clarke, Mulhall, Douglas *et al.* Role of extracellular membrane vesicles in the pathogenesis of various diseases, including cancer, renal diseases, atherosclerosis, and arthritis. *Lab. Invest.* **90**, 1549-1557 (2010).
7. Van der Pol, Edwin, Böing, Anita N *et al.* Classification, functions, and clinical relevance of extracellular vesicles. *Pharmacol. Rev.* **64**, 676-705 (2012).
8. Muralidharan-Chari, Vandhana, Clancy, James W *et al.* Microvesicles: mediators of extracellular communication during cancer progression. *J. Cell Sci.* **123**, 1603-1611 (2010).
9. de Candia, Paola, Torri, Anna *et al.* Intracellular modulation, extracellular disposal and serum increase of MiR-150 mark lymphocyte activation. *PloS one* **8** (2013).
10. Tanaka, Youhei, Kamohara, Hidenobu *et al.* Clinical impact of serum exosomal microRNA-21 as a clinical biomarker in human esophageal squamous cell carcinoma. *Cancer* **119**, 1159-1167 (2013).
11. Rabinowits, Guilherme, Gerçel-Taylor, Cicek *et al.* Exosomal microRNA: a diagnostic marker for lung cancer. *Clinical lung cancer* **10**, 42-46 (2009).
12. Nilsson, Jonas, Skog, Johan *et al.* Prostate cancer-derived urine exosomes: a novel approach to biomarkers for prostate cancer. *Br. J. Cancer* **100**, 1603-1607 (2009).
13. Hu, Shen, Arellano, Martha *et al.* Salivary proteomics for oral cancer biomarker discovery. *Clin. Cancer. Res.* **14**, 6246-6252 (2008).
14. Tong, Lingjun, Hao, Haining *et al.* Oral Administration of Bovine Milk-Derived Extracellular Vesicles Alters the Gut Microbiota and Enhances Intestinal Immunity in Mice. *Mol. Nutr. Food Res.* (2020).
15. Admyre, C, Telemo, E *et al.* Exosomes–nanovesicles with possible roles in allergic inflammation. *Allergy* **63**, 404-408 (2008).
16. Alexander, Margaret, Hu, Ruozhen *et al.* Exosome-delivered microRNAs modulate the inflammatory response to endotoxin. *Nature communications* **6**, 1-16 (2015).
17. Buzas, Edit I, György, Bence *et al.* Emerging role of extracellular vesicles in inflammatory diseases. *Nature Reviews Rheumatology* **10**, 356 (2014).
18. Gardiner, Chris, Ferreira, Yannick J *et al.* Extracellular vesicle sizing and enumeration by nanoparticle tracking analysis. *Journal of extracellular vesicles* **2**, 19671 (2013).
19. Nakamura, Yoshihiro, Miyaki, Shigeru *et al.* Mesenchymal-stem-cell-derived exosomes accelerate skeletal muscle regeneration. *FEBS Lett.* **589**, 1257-1265 (2015).
20. Candelario, Kate M & Steindler, Dennis A. The role of extracellular vesicles in the progression of neurodegenerative disease and cancer. *Trends Mol. Med.* **20**, 368-374 (2014).
21. Runz, Steffen, Keller, Sascha *et al.* Malignant ascites-derived exosomes of ovarian carcinoma patients contain CD24 and EpCAM. *Gynecologic oncology* **107**, 563-571 (2007).
22. Peinado, Héctor, Alečković, Maša *et al.* Melanoma exosomes educate bone marrow progenitor cells toward a pro-metastatic phenotype through MET. *Nat. Med.* **18**, 883 (2012).
23. Muralidharan-Chari, Vandhana, Clancy, James W *et al.* Microvesicles: mediators of

extracellular communication during cancer progression. *J. Cell Sci.* **123**, 1603-1611 (2010).
24. Rajendran, Lawrence, Honsho, Masanori *et al.* Alzheimer's disease β-amyloid peptides are released in association with exosomes. *Proceedings of the National Academy of Sciences* **103**, 11172-11177 (2006).
25. An, Kyongman, Klyubin, Igor *et al.* Exosomes neutralize synaptic-plasticity-disrupting activity of Aβ assemblies in vivo. *Molecular brain* **6**, 47 (2013).
26. Rajendran, Lawrence, Bali, Jitin *et al.* Emerging roles of extracellular vesicles in the nervous system. *J. Neurosci.* **34**, 15482-15489 (2014).
27. Logozzi, Mariantonia, De Milito, Angelo *et al.* High levels of exosomes expressing CD63 and caveolin-1 in plasma of melanoma patients. *PloS one* **4** (2009).
28. Yang, Tianzhi, Martin, Paige *et al.* Exosome delivered anticancer drugs across the blood-brain barrier for brain cancer therapy in Danio rerio. *Pharm. Res.* **32**, 2003-2014 (2015).
29. Yang, Tianzhi, Martin, Paige *et al.* Exosome delivered anticancer drugs across the blood-brain barrier for brain cancer therapy in Danio rerio. *Pharm. Res.* **32**, 2003-2014 (2015).
30. Chen, Jieli & Chopp, Michael Exosome therapy for stroke. *Stroke* **49**, 1083-1090 (2018).
31. Wang, Jinheng, Zheng, Yongjiang *et al.* Exosome-based cancer therapy: implication for targeting cancer stem cells. *Frontiers in pharmacology* **7**, 533 (2017).
32. Delcayre, Alain, Estelles, Angeles *et al.* Exosome display technology: applications to the development of new diagnostics and therapeutics. *Blood Cells, Molecules, and Diseases* **35**, 158-168 (2005).
33. Sheridan, Cormac, Exosome cancer diagnostic reaches market (Nature Publishing Group, 2016).
34. Santucci, Laura, Bruschi, Maurizio *et al.* Urine proteome biomarkers in kidney diseases. I. Limits, perspectives, and first focus on normal urine. *Biomarker insights* **11**, BMI. S26229 (2016).
35. Liang, Shu-Ling & Clarke, William Urine proteomic profiling for biomarkers of acute renal transplant rejection, in *The Urinary Proteome* 185-191 (Springer, 2010).
36. O'Driscoll, Lorraine Expanding on exosomes and ectosomes in cancer. *New Engl. J. Med.* **372**, 2359-2362 (2015).
37. Habuka, Masato, Fagerberg, Linn *et al.* The urinary bladder transcriptome and proteome defined by transcriptomics and antibody-based profiling. *PloS one* **10** (2015).
38. Hattori, Shinichi, Kojima, Keitaro *et al.* Detection of bladder cancer by measuring CD44v6 expression in urine with real-time quantitative reverse transcription polymerase chain reaction. *Urology* **83**, 1443. e1449-1443. e1415 (2014).
39. Nikitina, AS, Sharova, EI *et al.* Datasets for next-generation sequencing of DNA and RNA from urine and plasma of patients with prostate cancer. *Data in brief* **10**, 369 (2017).
40. Ploussard, Guillaume & De La Taille, Alexandre Urine biomarkers in prostate cancer. *Nature Reviews* **7**, 101 (2010).
41. Pisitkun, Trairak, Shen, Rong-Fong *et al.* Identification and proteomic profiling of exosomes in human urine. *Proceedings of the National Academy of Sciences* **101**, 13368-13373 (2004).
42. Im, Hyungsoon, Shao, Huilin *et al.* Label-free detection and molecular profiling of exosomes with a nano-plasmonic sensor. *Nat. Biotechnol.* **32**, 490 (2014).
43. Melo, Sonia A, Luecke, Linda B *et al.* Glypican-1 identifies cancer exosomes and detects early pancreatic cancer. *Nature* **523**, 177-182 (2015).
44. Peinado, Héctor, Alečković, Maša *et al.* Melanoma exosomes educate bone marrow progenitor cells toward a pro-metastatic phenotype through MET. *Nat. Med.* **18**, 883 (2012).
45. Yoshioka, Yusuke, Kosaka, Nobuyoshi *et al.* Ultra-sensitive liquid biopsy of circulating extracellular vesicles using ExoScreen. *Nature communications* **5**, 1-8 (2014).
46. Pisitkun, Trairak, Johnstone, Rose *et al.* Discovery of urinary biomarkers. *Molecular & Cellular Proteomics* **5**, 1760-1771 (2006).
47. Cranston, Joseph W, Perini, Fulvio *et al.* Purification and properties of ribonucleases from human urine. *Biochimica et Biophysica Acta (BBA)-Enzymology* **616**, 239-258 (1980).
48. Kooijmans, Sander AA, Vader, Pieter *et al.* Exosome mimetics: a novel class of drug delivery systems. *International journal of nanomedicine* **7**, 1525 (2012).

49. Jang, Su Chul, Kim, Oh Youn *et al.* Bioinspired exosome-mimetic nanovesicles for targeted delivery of chemotherapeutics to malignant tumors. *ACS nano* **7**, 7698-7710 (2013).
50. Tian, Yanhua, Li, Suping *et al.* A doxorubicin delivery platform using engineered natural membrane vesicle exosomes for targeted tumor therapy. *Biomaterials* **35**, 2383-2390 (2014).
51. Johnsen, Kasper Bendix, Gudbergsson, Johann Mar *et al.* A comprehensive overview of exosomes as drug delivery vehicles—endogenous nanocarriers for targeted cancer therapy. *Biochimica et Biophysica Acta (BBA)-Reviews on Cancer* **1846**, 75-87 (2014).
52. Ohno, Shin-ichiro, Takanashi, Masakatsu *et al.* Systemically injected exosomes targeted to EGFR deliver antitumor microRNA to breast cancer cells. *Mol. Ther.* **21**, 185-191 (2013).
53. Morse, Michael A, Garst, Jennifer *et al.* A phase I study of dexosome immunotherapy in patients with advanced non-small cell lung cancer. *Journal of translational medicine* **3**, 9 (2005).
54. Escudier, Bernard, Dorval, Thierry *et al.* Vaccination of metastatic melanoma patients with autologous dendritic cell (DC) derived-exosomes: results of thefirst phase I clinical trial. *Journal of translational medicine* **3**, 10 (2005).
55. Dai, Shengming, Wei, Dong *et al.* Phase I clinical trial of autologous ascites-derived exosomes combined with GM-CSF for colorectal cancer. *Mol. Ther.* **16**, 782-790 (2008).
56. Neumann, Eberhard, Schaefer-Ridder, M *et al.* Gene transfer into mouse lyoma cells by electroporation in high electric fields. *The EMBO journal* **1**, 841-845 (1982).
57. Hood, Joshua L, Scott, Michael J *et al.* Maximizing exosome colloidal stability following electroporation. *Anal. Biochem.* **448**, 41-49 (2014).
58. Jang, Su Chul, Kim, Oh Youn *et al.* Bioinspired exosome-mimetic nanovesicles for targeted delivery of chemotherapeutics to malignant tumors. *ACS nano* **7**, 7698-7710 (2013).
59. Bryniarski, Krzysztof, Ptak, Wlodzimierz *et al.* Antigen-specific, antibody-coated, exosome-like nanovesicles deliver suppressor T-cell microRNA-150 to effector T cells to inhibit contact sensitivity. *J. Allergy Clin. Immunol.* **132**, 170-181. e179 (2013).
60. Lee, Yeong Shin, Kim, Soo Hyun *et al.* Introduction of the CIITA gene into tumor cells produces exosomes with enhanced anti-tumor effects. *Experimental & molecular medicine* **43**, 281-290 (2011).
61. Yin, Weifan, Ouyang, Song *et al.* Immature dendritic cell-derived exosomes: a promise subcellular vaccine for autoimmunity. *Inflammation* **36**, 232-240 (2013).
62. Webber, Jason & Clayton, Aled. How pure are your vesicles? *Journal of extracellular vesicles* **2**, 19861 (2013).
63. Witwer, Kenneth W, Buzás, Edit I *et al.* Standardization of sample collection, isolation and analysis methods in extracellular vesicle research. *Journal of extracellular vesicles* **2**, 20360 (2013).
64. Lane, Rebecca E, Korbie, Darren *et al.* Analysis of exosome purification methods using a model liposome system and tunable-resistive pulse sensing. *Scientific reports* **5**, 7639 (2015).
65. Webber, Jason & Clayton, Aled How pure are your vesicles? *Journal of extracellular vesicles* **2**, 19861 (2013).
66. Zhu, Ling, Wang, Kun *et al.* Label-free quantitative detection of tumor-derived exosomes through surface plasmon resonance imaging. *Anal. Chem.* **86**, 8857-8864 (2014).
67. Im, Hyungsoon, Shao, Huilin *et al.* Label-free detection and molecular profiling of exosomes with a nano-plasmonic sensor. *Nat. Biotechnol.* **32**, 490 (2014).
68. Shang, Jing & Gao, Xiaohu Nanoparticle counting: towards accurate determination of the molar concentration. *Chem. Soc. Rev.* **43**, 7267-7278 (2014).
69. Heider, Susanne & Metzner, Christoph Quantitative real-time single particle analysis of virions. *Virology* **462**, 199-206 (2014).
70. Rupert, Deborah LM, Claudio, Virginia *et al.* Methods for the physical characterization and quantification of extracellular vesicles in biological samples. *Biochimica et Biophysica Acta (BBA)-General Subjects* **1861**, 3164-3179 (2017).
71. Sedmak, J James & Grossberg, Sidney E A rapid, sensitive, and versatile assay for protein using Coomassie brilliant blue G250. *Anal. Biochem.* **79**, 544-552 (1977).
72. Smith, PK etal, Krohn, R Il *et al.* Measurement of protein using bicinchoninic acid. *Anal.*

Biochem. **150**, 76-85 (1985).
73. Théry, Clotilde, Amigorena, Sebastian *et al.* Isolation and characterization of exosomes from cell culture supernatants and biological fluids. *Current protocols in cell biology* **30**, 3.22. 21-23.22. 29 (2006).
74. Wiechelman, Karen J, Braun, Robert D *et al.* Investigation of the bicinchoninic acid protein assay: identification of the groups responsible for color formation. *Anal. Biochem.* **175**, 231-237 (1988).
75. Cvjetkovic, Aleksander, Lötvall, Jan *et al.* The influence of rotor type and centrifugation time on the yield and purity of extracellular vesicles. *Journal of extracellular vesicles* **3**, 23111 (2014).
76. Xiao, Deyi, Ohlendorf, Joanna *et al.* Identifying mRNA, microRNA and protein profiles of melanoma exosomes. *PloS one* **7** (2012).
77. Vojtech, Lucia, Woo, Sangsoon *et al.* Exosomes in human semen carry a distinctive repertoire of small non-coding RNAs with potential regulatory functions. *Nucleic Acids Res.* **42**, 7290-7304 (2014).
78. Osteikoetxea, Xabier, Balogh, Andrea *et al.* Improved characterization of EV preparations based on protein to lipid ratio and lipid properties. *PloS one* **10** (2015).
79. He, Dinggeng, Wang, Huizhen *et al.* Total internal reflection-based single-vesicle in situ quantitative and stoichiometric analysis of tumor-derived exosomal microRNAs for diagnosis and treatment monitoring. *Theranostics* **9**, 4494 (2019).
80. Oosthuyzen, Wilna, Sime, Nicole EL *et al.* Quantification of human urinary exosomes by nanoparticle tracking analysis. *The Journal of physiology* **591**, 5833-5842 (2013).
81. Choi, Dong-Sic, Kim, Dae-Kyum *et al.* Proteomics of extracellular vesicles: exosomes and ectosomes. *PROTEOMICS–Clinical Applications* **34**, 474-490 (2015).
82. Pocsfalvi, Gabriella, Stanly, Christopher *et al.* Mass spectrometry of extracellular vesicles. *Mass Spectrom. Rev.* **35**, 3-21 (2016).
83. Rupert, Déborah LM, Lässer, Cecilia *et al.* Determination of exosome concentration in solution using surface plasmon resonance spectroscopy. *Anal. Chem.* **86**, 5929-5936 (2014).
84. Nolan, John P & Duggan, Erika Analysis of individual extracellular vesicles by flow cytometry, in *Flow Cytometry Protocols* 79-92 (Springer, 2018).
85. Moon, Pyong-Gon, Lee, Jeong-Eun *et al.* Fibronectin on circulating extracellular vesicles as a liquid biopsy to detect breast cancer. *Oncotarget* **7**, 40189 (2016).
86. Rupert, Déborah LM, Lässer, Cecilia *et al.* Determination of exosome concentration in solution using surface plasmon resonance spectroscopy. *Anal. Chem.* **86**, 5929-5936 (2014).
87. Théry, Clotilde, Boussac, Muriel *et al.* Proteomic analysis of dendritic cell-derived exosomes: a secreted subcellular compartment distinct from apoptotic vesicles. *The Journal of Immunology* **166**, 7309-7318 (2001).
88. Théry, Clotilde, Ostrowski, Matias *et al.* Membrane vesicles as conveyors of immune responses. *Nature reviews immunology* **9**, 581-593 (2009).
89. Dragovic, Rebecca A, Gardiner, Christopher *et al.* Sizing and phenotyping of cellular vesicles using Nanoparticle Tracking Analysis. *Nanotechnology, Biology and Medicine* **7**, 780-788 (2011).
90. Van Der Pol, E, Hoekstra, AG *et al.* Optical and non-optical methods for detection and characterization of microparticles and exosomes. *Journal of Thrombosis and Haemostasis* **8**, 2596-2607 (2010).
91. Gardiner, Chris, Ferreira, Yannick J *et al.* Extracellular vesicle sizing and enumeration by nanoparticle tracking analysis. *Journal of extracellular vesicles* **2**, 19671 (2013).
92. Alvarez-Erviti, Lydia, Seow, Yiqi *et al.* Lysosomal dysfunction increases exosome-mediated alpha-synuclein release and transmission. *Neurobiology of disease* **42**, 360-367 (2011).
93. Tomlinson, Paul R, Zheng, Ying *et al.* Identification of distinct circulating exosomes in Parkinson's disease. *Annals of clinical and translational neurology* **2**, 353-361 (2015).
94. Varga, Zoltán, Yuana, Yuana *et al.* Towards traceable size determination of extracellular vesicles. *Journal of extracellular vesicles* **3**, 23298 (2014).
95. Van Der Pol, E, Hoekstra, AG *et al.* Optical and non-optical methods for detection and

characterization of microparticles and exosomes. *Journal of Thrombosis and Haemostasis* **8**, 2596-2607 (2010).
96. Sharma, Shivani, Rasool, Haider I *et al.* Structural-mechanical characterization of nanoparticle exosomes in human saliva, using correlative AFM, FESEM, and force spectroscopy. *ACS nano* **4**, 1921-1926 (2010).
97. Sharma, Shivani, Gillespie, Boyd M *et al.* Quantitative nanostructural and single-molecule force spectroscopy biomolecular analysis of human-saliva-derived exosomes. *Langmuir* **27**, 14394-14400 (2011).
98. Palanisamy, Viswanathan, Sharma, Shivani *et al.* Nanostructural and transcriptomic analyses of human saliva derived exosomes. *PloS one* **5** (2010).
99. Palmieri, Valentina, Lucchetti, Donatella *et al.* Dynamic light scattering for the characterization and counting of extracellular vesicles: a powerful noninvasive tool. *J. Nanopart. Res.* **16**, 2583 (2014).
100. Atay, Safinur, Gercel-Taylor, Cicek *et al.* Morphologic and proteomic characterization of exosomes released by cultured extravillous trophoblast cells. *Exp. Cell Res.* **317**, 1192-1202 (2011).
101. Lawrie, AS, Albanyan, A *et al.* Microparticle sizing by dynamic light scattering in fresh-frozen plasma. *Vox Sang.* **96**, 206-212 (2009).
102. Cheng, Lesley, Sharples, Robyn A *et al.* Exosomes provide a protective and enriched source of miRNA for biomarker profiling compared to intracellular and cell-free blood. *Journal of extracellular vesicles* **3**, 23743 (2014).
103. Patko, D, Gyorgy, B *et al.* Label-free optical monitoring of surface adhesion of extracellular vesicles by grating coupled interferometry. *Sensors Actuators B: Chem.* **188**, 697-701 (2013).
104. Böing, AN, Stap, J *et al.* Active caspase-3 is removed from cells by release of caspase-3-enriched vesicles. *Biochimica et Biophysica Acta (BBA)-Molecular Cell Research* **1833**, 1844-1852 (2013).
105. Weatherall, Eva & Willmott, Geoff R Applications of tunable resistive pulse sensing. *Analyst* **140**, 3318-3334 (2015).
106. Akagi, Takanori, Kato, Kei *et al.* On-chip immunoelectrophoresis of extracellular vesicles released from human breast cancer cells. *PLoS One* **10** (2015).
107. Osteikoetxea, Xabier, Balogh, Andrea *et al.* Improved characterization of EV preparations based on protein to lipid ratio and lipid properties. *PloS one* **10** (2015).
108. Kanwar, Shailender Singh, Dunlay, Christopher James *et al.* Microfluidic device (ExoChip) for on-chip isolation, quantification and characterization of circulating exosomes. *Lab on a Chip* **14**, 1891-1900 (2014).
109. Logozzi, Mariantonia, De Milito, Angelo *et al.* High levels of exosomes expressing CD63 and caveolin-1 in plasma of melanoma patients. *PloS one* **4** (2009).
110. Palanisamy, Viswanathan, Sharma, Shivani *et al.* Nanostructural and transcriptomic analyses of human saliva derived exosomes. *PloS one* **5** (2010).
111. Patching, Simon G Surface plasmon resonance spectroscopy for characterisation of membrane protein–ligand interactions and its potential for drug discovery. *Biochimica et Biophysica Acta (BBA)-Biomembranes* **1838**, 43-55 (2014).
112. Van Der Pol, E, Van Gemert, MJC *et al.* Single vs. swarm detection of microparticles and exosomes by flow cytometry. *Journal of Thrombosis and Haemostasis* **10**, 919-930 (2012).
113. Stoner, Samuel A, Duggan, Erika *et al.* High sensitivity flow cytometry of membrane vesicles. *Cytometry* **89**, 196-206 (2016).
114. Tallarek, U, Rapp, E *et al.* Electroosmotic flow phenomena in packed capillaries: from the interstitial velocities to intraparticle and boundary layer mass transfer. *The Journal of Physical Chemistry* **106**, 12709-12721 (2002).
115. Kemp, Graham Capillary electrophoresis: a versatile family of analytical techniques. *Biotechnol. Appl. Biochem.* **27**, 9-17 (1998).
116. Kraly, James, Fazal, Md Abul *et al.* Bioanalytical applications of capillary electrophoresis. *Anal. Chem.* **78**, 4097-4110 (2006).
117. Mironov, Gleb G, Chechik, Alexey V *et al.* Viral quantitative capillary electrophoresis for

counting intact viruses. *Anal. Chem.* **83**, 5431-5435 (2011).
118. Azizi, Afnan, Mironov, Gleb G *et al.* Viral quantitative capillary electrophoresis for counting and quality control of RNA viruses. *Anal. Chem.* **84**, 9585-9591 (2012).
119. Moh'd Khushman, Arun Bhardwaj, Patel, Girijesh Kumar *et al.* Exosomal Markers (CD63 and CD9) Expression Pattern Using Immunohistochemistry in Resected Malignant and Non-malignant Pancreatic Specimens. *Pancreas* **46**, 782 (2017).
120. Théry, Clotilde, Witwer, Kenneth W *et al.* Minimal information for studies of extracellular vesicles 2018 (MISEV2018): a position statement of the International Society for Extracellular Vesicles and update of the MISEV2014 guidelines. *Journal of extracellular vesicles* **7**, 1535750 (2018).
121. Hoshino, Ayuko, Costa-Silva, Bruno *et al.* Tumour exosome integrins determine organotropic metastasis. *Nature* **527**, 329-335 (2015).
122. Wu, Jiayan, Xiao, Jingfa *et al.* Ribogenomics: the Science and Knowledge of RNA. *Genomics, proteomics & bioinformatics* **12**, 57-63 (2014).